People's Democratic Republic of Algeria
Ministry of Higher Education and Scientific Research
University M'Hamed Bougara Boumerdes
Faculty of Engineering

Department Of Industrial Maintenance
Engine's Dynamics and Vibroacoustics Laboratory

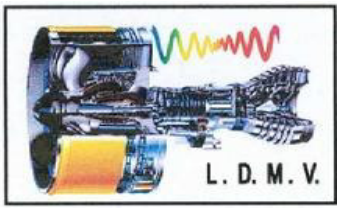

In Partial Fulfillment
of the Requirements for the Degree
Master in Mechanics and systems engineering

TOPIC

Static analysis of a smart sandwich beam subject to an extension force

Submitted by:

MAGHNINI Khaled

MEKIRI Abdelghani

Under the supervision:
Mr AGUIB salah

PROMOTION 2016/2017

ACKNOWLEDGEMENTS

First and foremost we would like to thank God for blessing us with the opportunity and ability to compete and succeed at such a challenging university.

We want to thank our advisor Mr. Salah Aguib for his invaluable guidance, motivation, constant inspiration and above all his ever co-operating attitude enabled us in bringing up this study in present elegant form.

It is a great pleasure for us to acknowledge and express our gratitude to our parents for their understanding unstinted support and endless encouragement during our studies.

We are greatly thankful to all the staff members of the department and all our well wishers, class mates and friends for their inspiration and help.

Lastly we sincerely thank to all those who have directly or indirectly helped for the work reported herein.

Abstract

The composite materials in magnetorheological elastomer (intelligent material) possess mechanical properties important. These materials are incorporated into mechanical structures such that the beams, plates and shells, these structures sandwiches in MRE are recently used in many industrial sectors because of their high flexural stiffness accompanied by strong energy dissipation. In this work we studied the static behavior of beam composed of a core in elastomer magnetorheological inserted between two skins in aluminum. To well understand the behavior of these structures there has developed a digital approach by the method of Ritz as well as a simulation by MEF under the Code of calculation ABAQUS, the results found are well face.

Keywords: magnetorheological elastomer, viscoelastic, sandwich beams, FEM

Résumé

Les matériaux composites en élastomère magnétorhéologique (matériau intelligent) possèdent des propriétés mécaniques importantes. Ces matériaux sont incorporés dans structures mécaniques tels que les poutres, les plaques et les coques, ces structures sandwiches en MRE sont récemment utilisées dans des nombreux secteurs industriels à cause de leur haute rigidité en flexion accompagnée d'une forte dissipation d'énergie. Dans ce travail on a étudié le comportement statique d'une poutre composée d'un core en élastomère magnétorhéologique inséré entre deux peaux en aluminium. Pour comprendre bien le comportement de ces structures on a développé une approche numérique par la méthode de Ritz ainsi que une simulation par MEF sous le code de calcul Abaqus, les résultats trouvés sont bien confrontés.

Mots clés Elastomère, Viscoélastique, Poutre sandwich, MEF

الملخص

المواد المركبة في المطاط الصناعي المغناطيسي (المواد الذكية) تمتلك الخصائص الميكانيكية هامة.هذه المواد قد ادرجت في الهياكل الميكانيكية مثل الدعامات, الصفائح, الهياكل, هذه الهياكل من طبقات اللزج المطاطي الممغنط تستعمل مؤخراً في العديد من القطاعات بسبب الصلابة العالية مصحوبا بارتفاع في امتصاص الطاقة. في هذا العمل نقوم بدراسة سكون الشطيرة تتالف من طبقة اللزج المطاطي الممغنط و طبقتين من الالممنيوم. و لفهم الجيد لسلوك هذه الهياكل تم تطوير نهج الرقمي لطريقة (ريتز) و كذالك بواسطة (ع ط م) تحت قانون حساب ABAQUS و النتائج التي حصلنا عليها متشابهة .

مفتاح الكلمات : لزج مطاطي ممغنط, دعامة مع الشطيرة, ط ع م

Nomenclature

Symbol	Name
σ (t)	stress
ε (t)	strain
G (t)	Shear relaxation modulus
C (t)	creep compliance of the viscoelastic material
G_∞	Equilibrium modulus
G_i	Relaxation strength
τ_i	Relaxation time
C_g	Glassy compliance
C_i	Retardation strength
ζ_i	Retardation time
$G^{'}(\omega)$	Storage function
$G^{''}(\omega)$	Loss function
$C_{crp}(t)$	Creep relaxation
$E_{rel}(t)$	Relaxation relation
τ	Shear stress
γ	Shear strain
G	Shear modulus
η	Viscosity
ω	Angular velocity
f	Frequency
u_i^0	Longitudinal displacement of the top layer
z_i	Distance from centroid of top layer
w_i	Transverse displacement in the top layer

w_i^0	Transverse displacement at the centroid of the top and bottom layer
u_2	Longitudinal displacement in the MRE
u_2^0	Longitudinal displacement at the centroid of the MRE
α	Shear deformation in MER core
β	Transverse normal deformation in MER core
h	Thickness of the beam
L	Length of the beam
U	Displacement
$\varphi_1 \dots \varphi_n$	Shape functions
$C_1 \dots C_n$	Coefficients of shape functions
m_{ij}	Matrix mass
K_{ij}	Stiffness matrix
K^{-1}	The inveres stiffness matrix
$G^*(t)$	Complex module
G'	The real part (module of conservation)
G''	The imaginary part (module of dissipation)
E	Elastic modulus
ν	Poisson's coefficient
B	intensity of magnetic field

LIST OF CONTENTS

LIST OF FIGURE

Chapter II

Chapter III

Chapter IV

LIST OF TABLES

General introduction

In order to improve the mechanical characteristics of the structures and the guard of the fatigue and the early break, it is essential to controls within their Mechanical properties and vibratory behavior. The importance of constructions (nuclear centrals, space structures …) is continuously increasing because of developing technology. Materials are generally accepted as elastic in engineering constructions due to calculation simplicity, but, used materials actually demonstrate a viscoelastic behavior, so, models which give the actual behavior of material with more time consuming computing capacity should be used for more precise determination of behavior of materials used in constructions, this requires vescoelastic material assumptions instead of the use of elastic material assumptions. Under normal conditions, in metals, the modulus of elasticity can be modeled as a constant, that is, the modulus of elasticity is not treated as a function of frequency in dynamic models [1].

Magneto-rheological (MR) materials exhibit rapid variations in their rheological properties such as viscosity and shear modulus when subjected to different magnetic field intensities. Since is it discovery by Rabinow in 1948. Magnetorheological materials have developed into a family with Magneto-rheological fluid, Magneto-rheological foam and Magneto-rheological elastomer [2]. The most common Magneto-rheological material is Magneto-rheological fluid (MRF). The general criterion to estimate the MR effect of MRF is the variation capability of dynamic yield stress within a post-yield regime under external applied magnetic field. A lot of applications based on MRF benefit from the properties that the dynamic yield stress can be continuously, rapidly and reversibly controlled by the applied magnetic field.

For viscoelastic materials, the modulus of elasticity can be assumed to be constant for static forces and variable forcing function, however, when viscoelastic materials undergo excitations from a random or transient forcing function the constant modulus of elasticity assumption may not be valid, this is because the second order equation of motion has non-constant coefficient that vary as a function of Mechanical properties Where the stress and strain of the plate are calculated by the finite element method. ZG Ying and al [3] studied forced of a magnetorheological elastomer sandwich by a random excitation plate where the responses of the plate are determined by the Galerkin method it has been observed from the available literature that though many works have been reported on the deformation analysis of MRE embedded viscoelastic cored

sandwich beam simply supported, similarly, many researchers studied the parametric instability regions of sandwich beam with viscoelastic core with a patch MRE [4].

The present work provides an analysis on how magnetic fields change the dynamic property of the MRE embedded viscoelastic cored sandwich beam with conductive skins, consequently, reducing the levels of deformation of structures. Extensive researches are being conducted at the laboratory of structures in this subject. In the viscous fluid the mechanical energy is dissipated in the form of heat and in elastic solid the energy is stored in the form of strain energy, this combination of properties makes the vescoelastic material to behave uniquely, such in addition to undergoing instantaneous strain is also undergoes creep after the application of variable load.

CHAPTER I

Generalities of viscoelastic and magnetorheological elastomer materials

I.1. Introduction

In the present work, experimental and numerical analysis of the dynamics and damping propertics of a magnetorheological elastomer embedded viscoelastic cored sandwich beam is considered. The material functions of the viscoelastic core with a MRE patch are first determined in order to obtain the required data to characterize the material. Then, a parameter estimation method is considered for determining the appropriated parameters of the Maxwell generalized model for linear viscoelasticity.

In this chapter we studied some of the characteristics and classification of smart materials, and the latter are used in many fields and have many applications.

In general usage, the term elastomer means a group of polymers characterized by large deformability, time dependent (viscoelastic) behavior and considerable changes in material behaviour by temperature. Further properties of elastomers include a stress-strain curve demonstrating strongly strain-rate dependent non-linear characteristics and incompressibility, making it really difficult for engineers to determine the dimensions of structural components made of them. In spite of innumerable problems,

I.2. Generalists of viscoelastic material

I.2.1. Definition

Viscoelastic materials are named by their ability to display both viscous and elastic behavior. Whenever a body is subjected to an external force or deformation, the body responds by rearrangements of its microscopic constituents. In idealized viscous fluids, the time required for the rearrangement is assumed to be infinitely small. For ideally elastic solids, the time is assumed to be infinitely long. However, in any physical material, these rearrangements must take some finite time. Hence, most real-life materials demonstrate some viscoelastic properties. These effects may be particularly important when considering synthetic polymers or biological materials such as muscles or soft tissue. For a more thorough introduction to viscoelastic behavior and modeling than the material presented here, the monographs provide ample material. The history of viscoelastic modeling dates back to the last half of the nineteenth century and the works of Boltzmann, Kelvin, Maxwell and Weichert. The two main characteristics of viscoelastic behavior are the stress response of the material under an induced strain relaxation, and the strain response of the material under an induced stress: creep or retardation. Different materials can thus be identified by their

relaxation and creep response. To make ideas more concrete, consider a body of some material and the situation where a force is applied to a part of the boundary, kept constant for some time, and then removed**.** [5]

I.2.1.1. Viscous materials

Like honey, resist shear flow and strain linearly with time when stress is applied like Newtonian Liquid, fig.I.1.

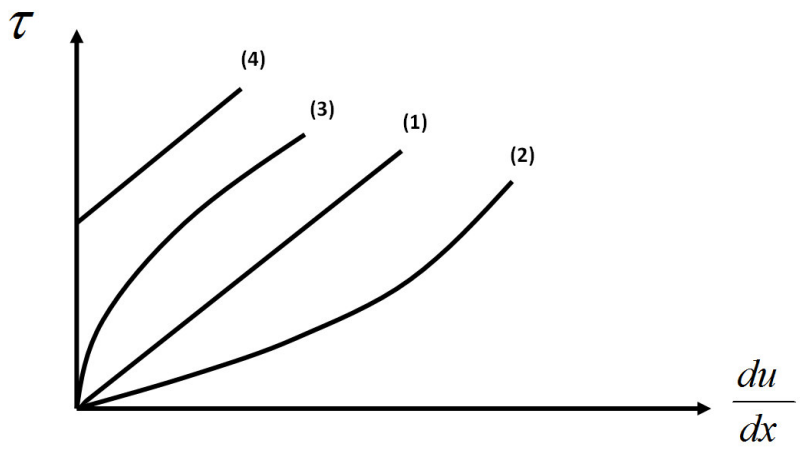

Figure.I.1.defferent types of response to a change in strain rate

(1) –Newtonian fluid (3) –Pseudo-plastic fluid

(2) –Dilatants fluid (4) –Bingham fluid

I.2.1.2. Elastic materials

Strain when stretched and quickly return to their original state once the stress removed like aluminum Stress versus strain in the viscous solid in loading and unloading process as figure I.2

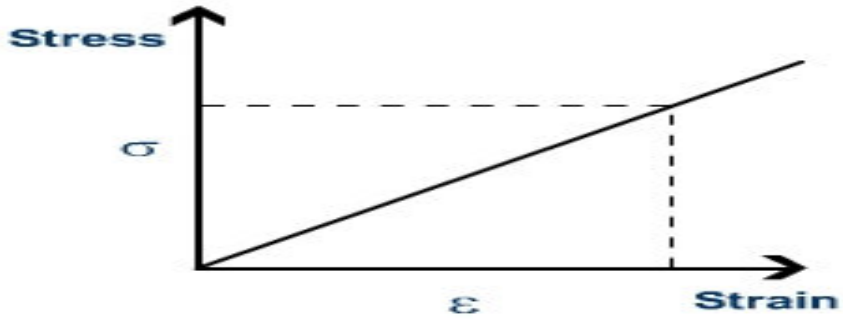

Figure.I.2. stress-strain curve for viscoelastic material in loading and unloading cycle

The curve of both viscous and elastic material in loading and unloading cycle.figure.I.3

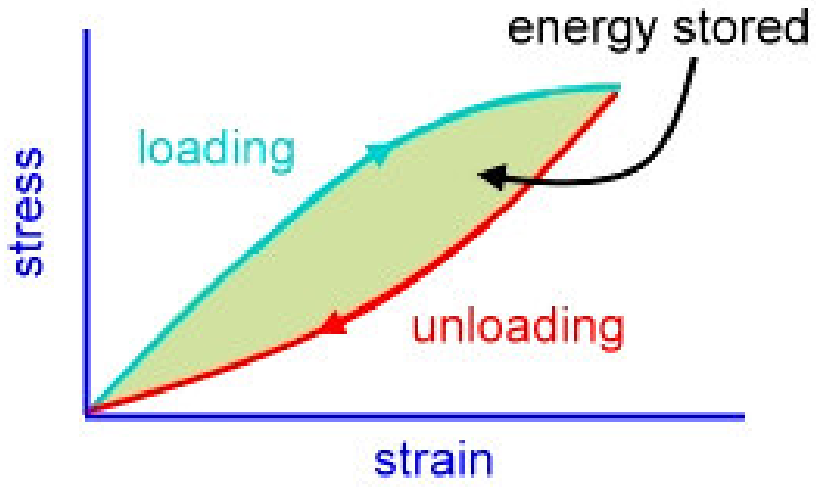

Figure.I.3. stress-strain curve for viscoelastic material

The red area is a hysteresis loop and showns the amount of energy lost in loading and unloading cycle

I.2.2. Mathematical Modeling of Linear Viscoelasticity

The uniaxial, non-aging and isothermal stress-strain equation for a linear viscoelastic material can be represented by a Boltzmann superposition integral,

$$\sigma(t) = \int_0^L G(t-\tau)\frac{d\varepsilon(\tau)}{d(\tau)}d\tau \tag{I.1}$$

$$\varepsilon(t) = \int_0^1 G(t-\tau)\frac{d\sigma(\tau)}{d(\tau)}d\tau \tag{I.2}$$

Where σ (t) and ε (t) stands for stress and strain, respectively, G (t) is the shear relaxation modulus and C (t) is the creep compliance of the viscoelastic material.

Different mechanical models, composed of springs and dampers, are provided in the literature in order to modeling the relaxation modulus and the creep compliance of viscoelastic materials.

The generalized Maxwell model or Wiechert model, which consists of a spring and (n) Maxwell elements connected in parallel, results in the following Prony series for the relaxation modulus

$$G(t) = G_\infty + \sum_{j=1}^{n} G_i e^{-t/\tau_i} \tag{I.3}$$

Where G_∞ is the equilibrium modulus, G_i and τ_i are the i-th relaxation strength and relaxation time, respectively.

The creep compliance, on the other hand, can be characterized more easily using the generalized Voigt model or Kelvin model,

Which consists of a spring and a dashpot and (n) Voigt elements connected in series, this model yields the creep compliance given by

$$C(t) = C_g + \sum_{i=1}^{n} C_i \left(1 + e^{-t/\zeta_i}\right) \tag{I.4}$$

Where C_g is the glassy compliance, C_i and ζ_i are the i-th retardation strength and retardation time, respectively.

Considering Eq. (I.3), the corresponding relaxation function in the frequency domain may be obtained

$$G(\omega) = G + jG''(\omega) \tag{I.5}$$

Where, $j = \sqrt{-1}$, $G'(\omega)$ is the storage function and $G''(\omega)$ is the loss function, given by

$$G'(\omega) = G_\infty + \sum_{i=1}^{n} \frac{\omega^2 \tau_i^2 G_i}{\omega^2 \tau_i^2 + 1} \tag{I.6}$$

$$G''(\omega) = \sum_{i=1}^{n} \frac{\omega^2 \tau_i^2 G_i}{\omega^2 \tau_i^2 + 1} \tag{I.7}$$

Therefore, for a given viscoelastic material, an inverse problem of parameter identification may be defined in order to fit the material functions in Eq. (I.3-I.5) to a set of experimental data.

I.2.3.Viscoelastic tensile tests

The behavior of viscoelastic material under axial load can be explained with superposition of elastic and viscose elements. While elastic behavior is modeled by means of a simple spring (Hooke model), viscose behavior is modeled by means of a dashpot (Newton model).

The most commonly viscoelastic tensile tests encounters only three (creep, stress relaxation and dynamic loading)

I.2.3.1. Creep test

It consists of measuring the time dependent strain from the application of steady uniaxial stress fig.I.4

The characteristics of creep function ideally should increase with time and converge to a steady state final value.

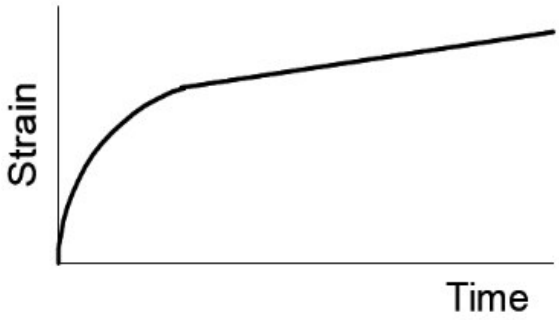

Figure.I.4.creep test curves

I.2.3.2. stress relaxation test

It consists of monitoring the time dependent stress resulting from a steady strain fig.1.5

The characteristics of relaxation function ideally should decrease with time and converge to a steady state final value.

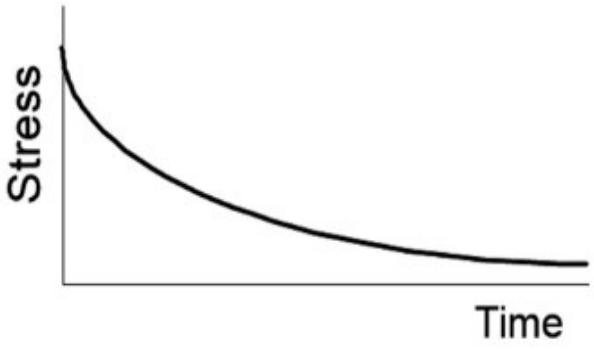

Figure.1.5. stress relaxation test curves

I.2.3.3. Dynamic loading test

For viscoelastic materials, the modulus of elasticity can be assumed to be constant for static forces and sinusoidal forcing function, however, when viscoelastic material undergo

excitations from a random or transient forcing function the constant modulus of elasticity assumption may not be valid. This is because the second order equation of motion has non-constant coefficients or coefficients that very as a function of frequency. Creep and relaxation tests are convenient for studying materiel response at long times (minutes or days) but less accurate at short times (second or less) dynamic test resulting from a sinusoidal strain (or stress are after well suited filling out the “short time" rang of response figure.I.6

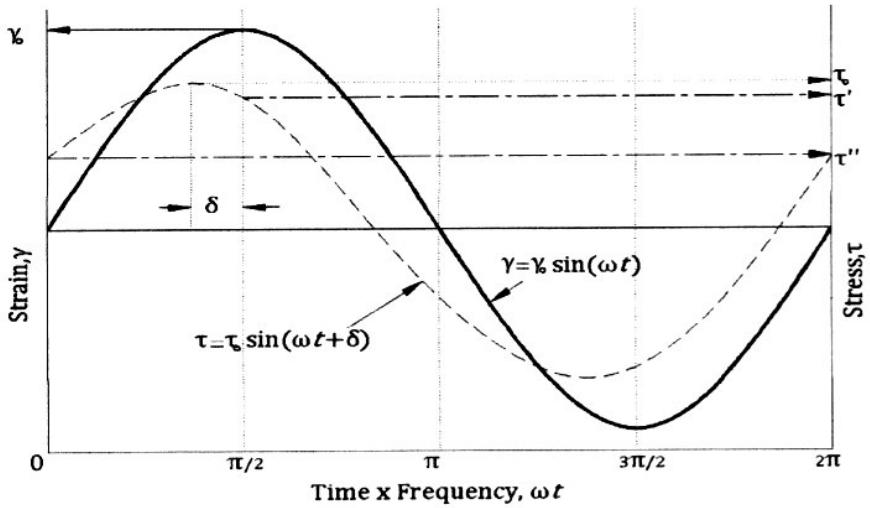

Figure.I.6. sinusoidal resulting of dynamic loading test

We can observe that, the strain in viscoelastic material is retarded in phase by an angle δ

I.3.Viscoelastic Sandwich Beam

For damping treatment with viscoelastic materials Grootenhuis summarized prior research. There are mainly two types of surface damping treatment: unconstrained and constrained. In the unconstrained layer treatment, a layer of viscoelastic material is applied with adhesive to the surface of structure. The energy is dissipated by the cyclic tensile and compressive strain when structure is in bending motion. In the case of constrained layer treatment, a stiff layer is added with adhesive to the top surface of viscoelastic layer so that the viscoclastic layer is sandwiched between the main base structure and elastic top layer. In this case, when the sandwich structure undergoes bending motion, the constrained layer causes significant shear deformation in the viscoelastic layer. The constrained layer damping trcatment is more efficient because the viscoelastic materials dissipate energy mainly by the shear deformation and the constrained layer augments the magnitude of shear deformation significantly. A constrained layer beam is comprised of two elastic layers separated by a viscoelastic core layer. fig.1.7

Elastic layer (aluminium)
Viscoelastic layer
Elastic layer (aluminium)

FigureI.7.sandwich layer beam

I.4. Viscoelasticity Models

To comprehend the effect of mechanic behavior of viscoelastic material and to represent it mathematically, the need of specific mechanical analog model arises.

Simplest way to capture both elastic and relaxation nature of polymers is by developing a model consisting of both elastic solid and viscous fluid dashpot.

These mechanical analogs use "hookian" spring depicted in figure.I.8 and described by $\sigma = \frac{E_c}{\varepsilon}$

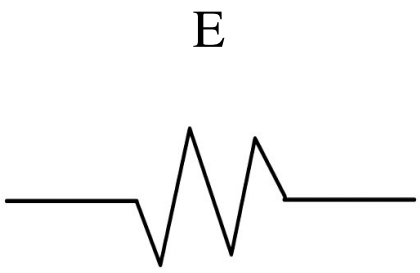

Figure.I.8. Hookean spring

The viscous part can be modeled a “Newtonian” deshpot (damper) shown in figure I.9 in which the stress produce by strain rate $\sigma = \eta\dot{\varepsilon}$

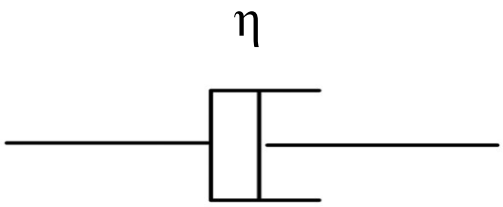

Figure.I.9. Newtonian dashpot

Various models with different combinations of solid and viscous fluid dashpot have been developed and here in the following we will briefly discuss Maxwell, Voigt, Zener Models known as Standard Solid Models,

I.4.1. Maxwell model

The spring and damper elements can be arranged in different variations depending on the material or structure to be modeled. For example, viscoelastic liquids can be approximated using a spring and dashpot in series. This model is known as the Maxwell element and is illustrated in Figure.I.10.

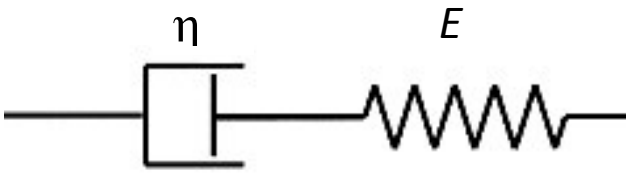

Figure I.10. Schematic representation of Maxwell model

I.4.2. Voigt model

The spring and damper (dashpot in parallel) is known as the Voigt model and can be used to approximate a viscoelastic solid. The Kelvin-Voigt model, illustrated in Figure.I.11 is the simplest model for a viscoelastic material.

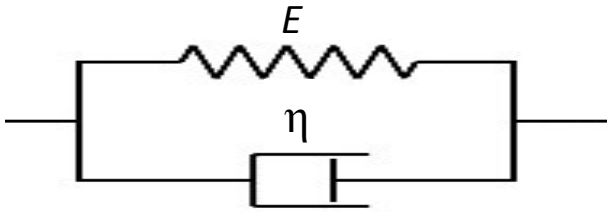

Figure I.11. Schematic representation of voigt model

I.4.3. Zener Model

In Zener model, two clastic springs are attached with a single dashpot in serial and parallel combination. Figure 1.12

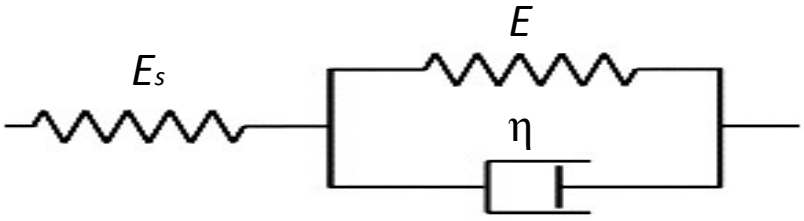

Figure.I.12. schematic representation of zener mode

I.4.4. Standard linear Solid (SLS)

Placing a spring parallel with the Maxwell unit gives a very useful model shown in fig.I.13 this spring has stiffness K_e so nomed because it provides an equilibrium or rubbery stiffness.

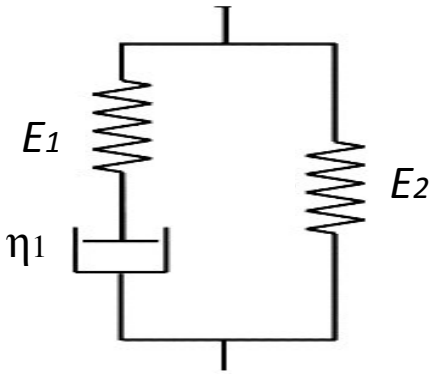

Figure.I.13. (SLS) model

I.4.5. Generalized Maxwell model

A Biot model is a variation of the generalized Maxwell model where the linear Viscoelastic damper in parallel is omitted from the generalized Maxwell model. A Biot model consists of a linear spring in parallel with an infinite number of Maxwell elements. Figure. I.14 depicts the Biot model.

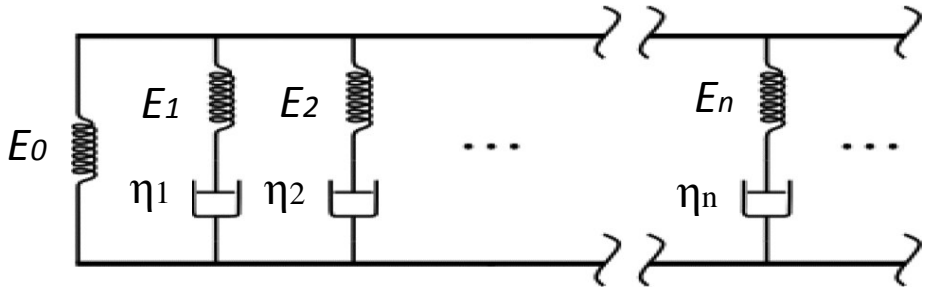

Figure.I.14. generalized Maxwell model

The classic models presented here can be used as building blocks when developing a model for damped structures and viscoelastic materials if the forcing function is sinusoidal and known. If the forcing function is random, transient, or unknown, both the stiffness and damping properties should be treated as a function of frequency

Figure.I 15 describes the time history of the creep functions of the above discussed three models

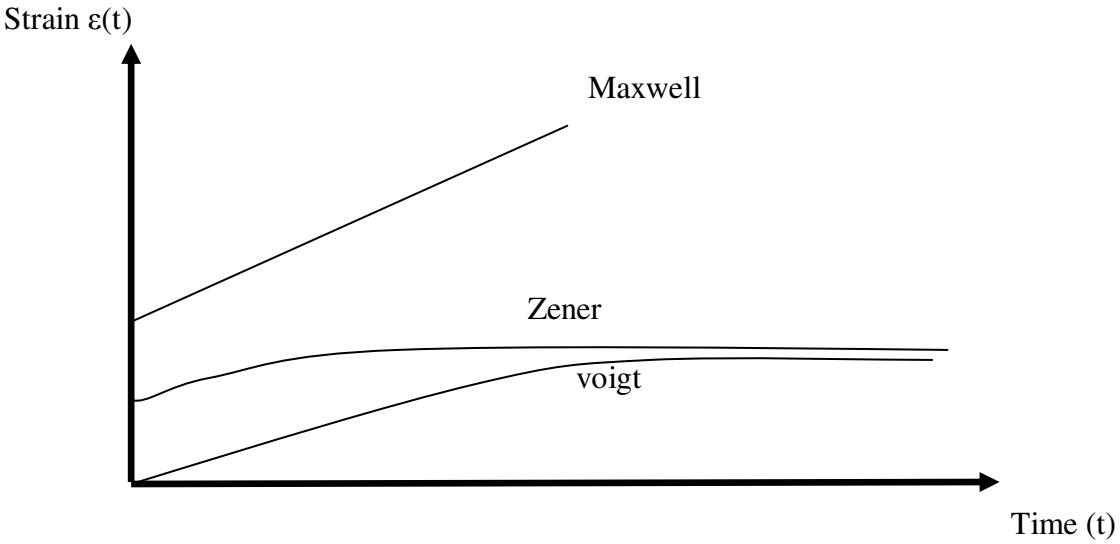

Figure. I.15. creep function for three models

We can observe that the creep function predicted by the Maxwell model, it does not converge to steady state value but keep on increasing with time.

And figure I.16 describes the time history of the relaxation function of the above discussed three models.

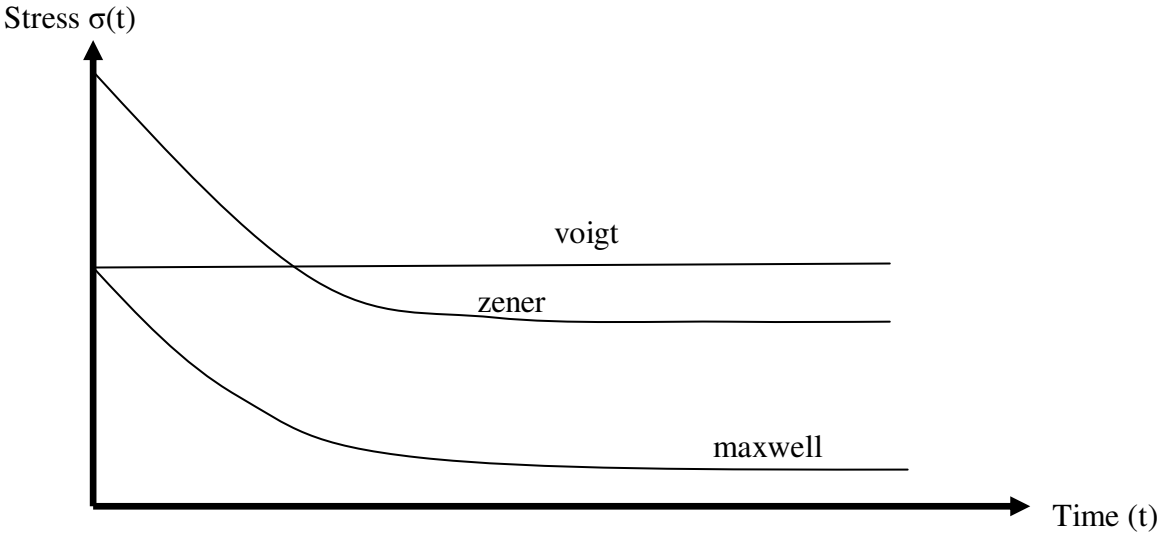

Figure.I.16. relaxation function for three models

We can observe that relaxation function predicted by the Voigt model impractical. It keeps constant throughout the time.

Table.I.1.viscoelastic material models and their mechanical properties

	Maxwell model	**Zener model**	**Voigt model**
Creep relaxation	$C_{crp}(t)=\frac{1}{E_1}+\frac{1}{E_v}t$	$C_{crp}(t)=\frac{1}{E_1}\left(1+\exp\left[-\frac{E_1}{E_v}t\right]\right)$	$C_{crp}(t)=\frac{1}{E_2}\exp\left[-\frac{E_1}{E_v}t\right]+\frac{1}{E_1}\left(1-\exp\left[-\frac{E_1}{E_v}t\right]\right)$
relaxation relation	$E_{rel}(t)=E_1\exp\left[-\frac{E_1}{E_v}t\right]$	$E_{rel}(t)=E_1\left(1-\exp\left[-\frac{E_1}{E_v}t\right]\right)$	$E_{rel}(t)=E_2\exp\left[-\frac{E_1}{E_v}t\right]+E_1\exp\left(1-\exp\left[-\frac{E_1}{E_v}t\right]\right)$

I.5. Smart materials

I.5.1. Generality

Smart or intelligent materials are material that has to respond to stimuli and environmental changes and to activate their function according these changes. The stimuli like a temperature, pressure, electric flow, and magnetic flow, light, mechanical, etc can originate internally or externally. Smart materials and related technologies have been drawing an increasing amount of attention from researchers in related fields worldwide. In the past decade, smart materials and structures has been one of the most progressive fields of research. Recently developed materials and devices have been used to address many challenges in aerospace, mechanical, bionics and medical technologies. The progress made in developing advanced materials and devices is impressive and encouraging. The theme of this special section is smart actuators and applications. This is one of the research areas of smart materials and structures that is recognized as an essential aspect of smart technologies. Therefore, we have organized this special section to promote the development of technology as well as international communication in this field. In the section, current progress in the field of smart materials and structures is presented. The papers published cover the most recent research results in the development of several different kinds of smart materials (e.g. fiber-reinforced shape memory polymer composites, electro-rheological fluids, electro-active papers, shape memory alloys etc) [6]**.** In addition, applications of the materials in smart structures are also included. We believe that the papers published in this special section will

be found to provide the latest information and will encourage more researchers to make their contribution to this field of research.

I.5.2. Properties of smart materials

- Sensing material and devices.
- Actuation material and devices.
- Control devices and techniques.
- Self detection, self diagnostic.
- Self corrective, self controlled, self healing.
- Shock absorber arrest.[7]

I.5.3. classification of smart material

Smart material can be grouped into the following categories:

I.5.3.1. Pizoelectric materials: when subjected to an electric or variation in voltage, piezoelectric material will undergo some mechanical change, and vice versa, these events are called the direct and converse effects. [7]

I.5.3.2. electrostrictive materials: This material as the same properties as piezoelectric material, but the mechanical change is proportional to the electric filed. These characteristic will always produce displacements in the same direction. [7]

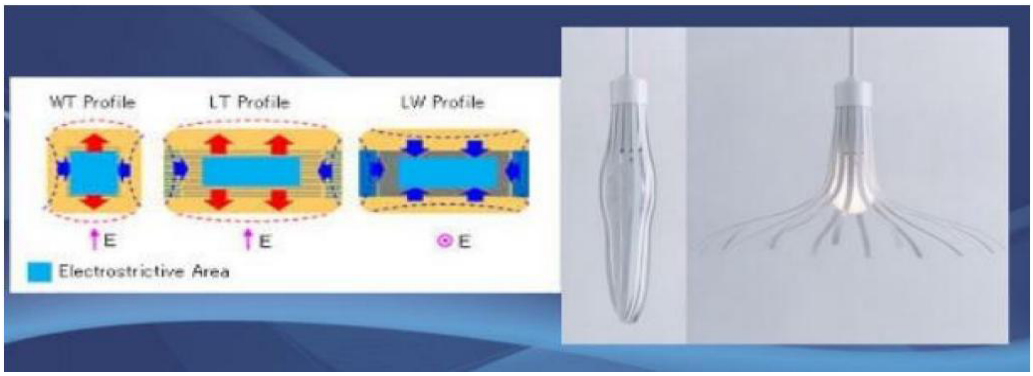

Figure.I.17. electrostrictive material

I.5.3.3. Magnetostrictive materials: when subjected to a magnetic field, and vice versa, this material will undergo and induced strain. Consequently, it can be used as a sensors and actuators

Figure.I.18. magnetostrictive materials

I.5.3.4. Rheological materials: These are in liquid phase which can change state instantly through the application of an electric or magnetic charge. These fluids may find application in brakes, shock absorber and damper for vehicle seats.

I.5.3.5. Thermoresponsive material: Thermoresponsive is the ability of the material to change properties in response to changes in temperature. They are useful in thermostat and parts of automotive and air vehicles

I.5.3.6. fullerences: These are spherically caged molecules with carbon atoms at the corner of structure consisting of pentagons and hexagons, These are usually used in polymeric metrices fur used in smart systems. They are used in electronic and microeiectronic devices.

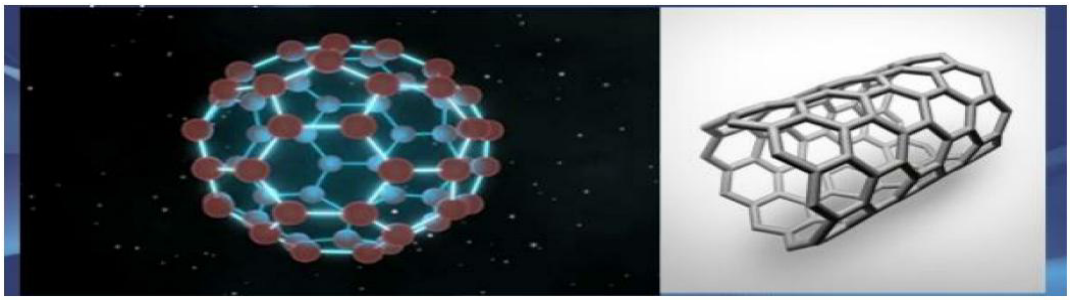

Figure.I.19. fullerences

I.6. Magnetorheological elastomer viscoelastic beam

I.6.1. Generality

Mgnetorheogical elastomers (MRE) belong to the new group of the functional materials called “smart”. Although smart materials are known since long time, the term smart materials.

Intelligent materials or less frequently used adaptive materials or multifunctional materials, was introduced in the eighties of the twentieth century, when some materials, which included in the group were already known.

Magnetorheological materials can be fluid, gel or even a solid material such as an elastomeric. Magnetorheological materials have magnetically polarisable colloidal particles suspended in some functional suspension, i.e. viscous fluid (silicone oil) or elastomeric matrix (silicone rubber).A magnetorheological fluid operates on the principle that the magnetic particles are randomly distributed in the liquid when no magnetic field is applied, but then the particles acquire a magnetic polarization and form chains in the presence of a magnetic field of sufficient strength, as indicated in the figure 1.20. The strength of this chain is dependent on the magnetic field density. Following from this, it is the strength of the particle chains which determines the increase in rheological properties for the fluid.

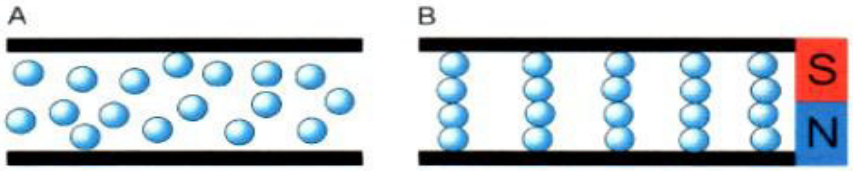

Figure.I.20. Magnetorheological material A-before-and after the application of an external magnetic field

I.6.2 Viscoelastic Properties of MRE

Many materials, especially polymers and their composites are characterized by viscoelastic properties. This means that they combine the features of elastic solids and viscous liquids, as schematically shown in figure1.21. Their behaviour is between the ideal solid described by Hook's law, in which the stress is always directly proportional to the strain and in independent of strain rate, and a viscous liquid, in which according to Newton's law, stress is always directly proportional to the strain rate and does not depend on the strain. Viscoelastic materials under rapid deformation behave more like elastic body, and under very slow as viscous liquid. Rheology describes the flow and deformation of solids and liquids under the influence of an external force.

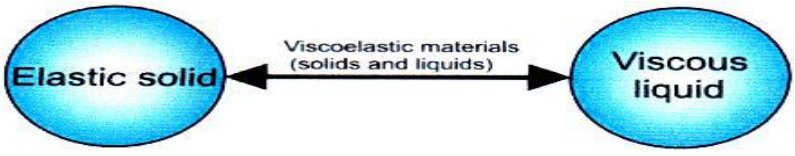

Figure.I.21. Viscoelastic proprties of materials

For a perfectly elastic solid when the force is applied, strain occurs immediately, and it is linearly proportional deformed body immediately returns to its initial state. The applied force can cause the shear stress (τ) and shear modulus (G). G modulus determines the resistance of the solid to deformation and is expressed by the ratio of shear stress (τ) to the shear strain (γ):

$$G = \frac{\tau}{\gamma} \tag{I.8}$$

For an elastic solid, both stress and strain are independent on time. For the viscoelastic solid, rheological parameters are dependent on the time and described by Kelvin-Voight model for linear viscoelasticity:

$$\tau = G\gamma + \eta \frac{d\gamma}{dt} \tag{I.9}$$

Where:

η: dynamic viscosity,

t: time.

Deformed material can undergo relaxation when the applied force in maintained, which results in a decrease in the stress in time, until is complete disappeared, as schematically shown in Figure.I.22. When the force is removed, the disappearance of deformation is delayed.

This delay is given by the relaxation time λ:

$$\lambda = \frac{\eta}{G} \tag{I.10}$$

In the area of the linear viscoelasticity delay times during creep and recovery are the same. Usually solids are more complicated and to describe the viscoelastic behaviour during the creep and recovery it is necessary to use the whole spectrum of relaxation times. In most testing methods of viscoelastic materials, instead of constant stress, dynamic strain measurements in the form of an oscillating sinusoidal function of time is used Fig.I.23

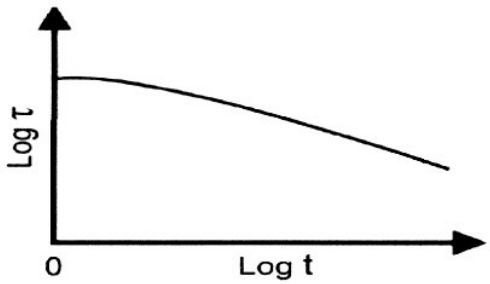

Figure.I.22. stress relaxation (τ) at time (t)

$$\tau = \tau_0 . \sin(\omega t) \quad \text{(I.11)}$$

Where: τ_0 - applied stress,

ω - Angular velocity [1/s or rad/s]

ω - 2πf (I.12)

f - Frequency [Hz]

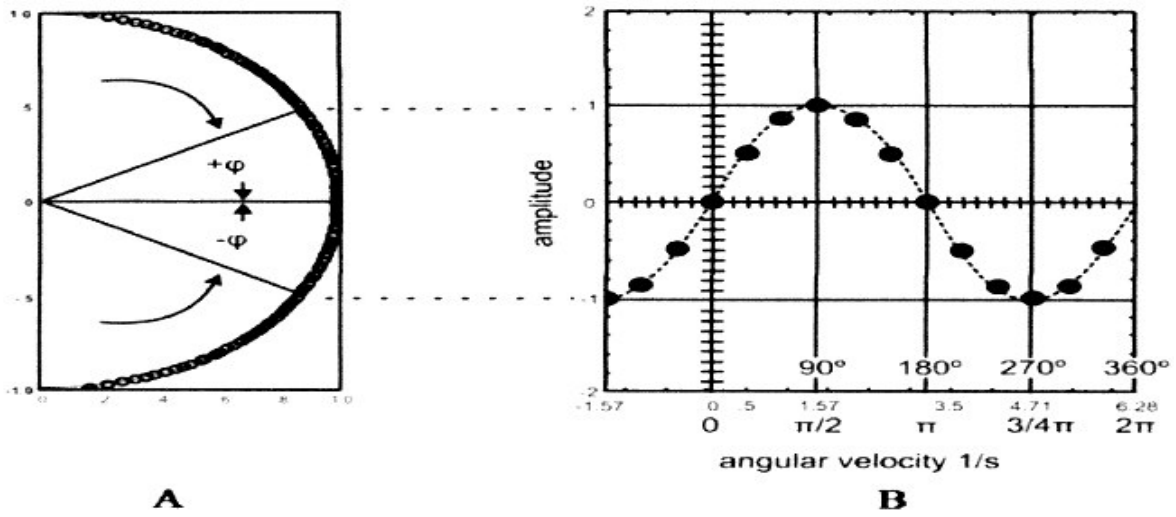

Figure.I.23. dynamic measurements: A - deformation of the angle φ, B – sinusoidal strain or stress

I.6.3.Applications of MRE

Due to the dynamic damping of Magnetorheological Fluids, much research has gone into their development for use in shock absorbers, clutches and brakes. These MRF's are also being developed as an innovative micro-machining method where abrasives are bonded to the ferromagnetic particles and the magnetic field is used to polish optical glass, ceramic and other brittle materials of millimetre or sub-millimeter scale whith a high efficiency [8]. Applications for Magnethorheoligical Elastomers include automotive bushings and engine

mounts [9], where the significant changes in spring rate due to an applied magnetic field can be used to control stiffness. Ferromagnetic composites have also found many applications in sensors, converters and controlled vibration dampers [10], however their manufacture is not yet widespread with standards for production.

There is some interest in developing soft, high strain materials as artificial muscles [11]. One possibility is elastomers filled with magnetic particles. When placed in a uniform magnetic field, such materials will tend to contract, an effect called magnetostiction. This contraction is due to the dependence of the composite susceptibility increasing along the direction of compression (in contrast, demagnetizing field can cause a material to elongate)

I.7. Generalized Maxwell model

A real polymer does not relax with a single relaxation as predicted by the previous models this loods to a distribution of relaxation times.

The generalized maxwell model in figure.I.24 can have as many spring-dashpot maxwell elements as are needed to approximate the distribution satisfactorily.

The behavior of linear viscoelastic material can be generally predicted using the generalized Maxwell model simulate the relaxation occurring at a distribution of times by the use of multiple numbers of spring and dashpot.

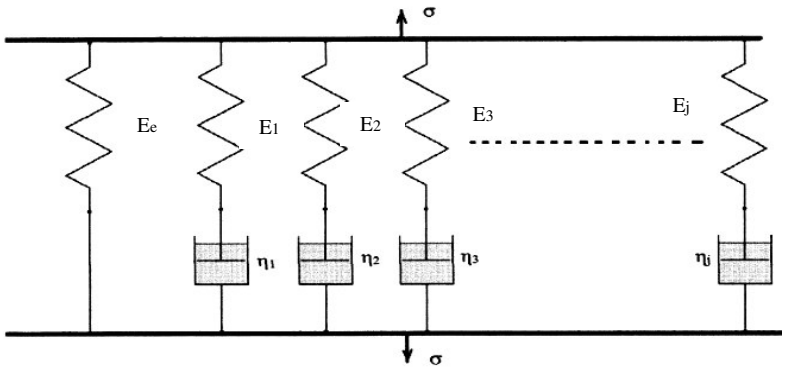

Figure.I.24. generalized Maxwell model

The total stress transmited by the model is the stress in the isolated spring (of stiffness E_e) plus that in each of the dashpot arms

$$\sigma = \sigma_e + \sum_j \sigma_j \qquad \text{(I.13)}$$

The stress in the maxwell arm is:

$$\bar{\bar{\sigma}} = \frac{E_j s \bar{\bar{\varepsilon}}}{s + \frac{1}{\tau_j}} \tag{I.14}$$

Then

$$\bar{\bar{\sigma}} = \bar{\bar{\sigma}}_e + \sum\nolimits_j \sigma_j = \left[E_e + \sum\nolimits_j \frac{E_j s}{s + \frac{1}{\tau_j}} \right] \bar{\bar{\varepsilon}} \tag{I.15}$$

The result can be written

$$\bar{\bar{\sigma}} = \zeta . \bar{\bar{\varepsilon}} \tag{I.16}$$

Where

$$\zeta = \left[E_e + \sum\nolimits_j \frac{E_j s}{s + \frac{1}{\tau_j}} \right] \tag{I.17}$$

The equation.I.16 reminiscent the hook's low $\sigma = E\varepsilon$ but in the Laplace plane is called (the associated viscoelastic constitutive equation)

I.8. Conclusion

The behavior of a viscoelastic structure is intermediate between that of an ideal elastic solid and that of a viscous liquid

Our materiel is constrained layer beam is comprised of two elastic layers separated by a viscoelastic core layer. The top and the bottom layer is aluminum and the core layer is the magnetoreologic elastomer, we choose it for magnetic field tests. A magnetorheologic elastomer operates on the principle that the magnetic particles are randomly distributed when no magnetic field is applied, but then the particles acquire a magnetic polarization and form chains in the presence of a magnetic field of sufficient strength.

Creep function predicted by the Maxwell model, it does not converge to steady state value but keep on increasing with time. The behavior of linear viscoelastic material can be generally predicted using the generalized Maxwell model for n spring and dashpot.

II.1. Introduction

It is very important to study the static behaviour of MRE for predict the statement of stiffness and damping in the structure

In this research work static analysis of a MRE sandwich beam has been studied. A Ritz method model has been developed for the three layer MRE sandwich beam

II.2. mathematical formulation

The sandwich beam model described here based on the following assumptions:

Top and bottom layers are considered as ordinary beams with axial and bending resistance.

The core layer carries negligible longitudinal stress, but takes the non linear displacement fields in x and z directions.

Transverse displacements of top and bottom layers equal transverse displacement of core at.

The sandwich beam considered here consists of three layers with viscoelastic material as a core layer, the top and bottom layers are isotropic and linear elastic material with thickness h_1 and h_3. The magnetorheological elastomer (MRE) core layer has a thickness of h_2, the complex shear modulus in the form of $G_c = G' + iG''$. The model of the magnetorheological sandwich beam has shown in the figure given below

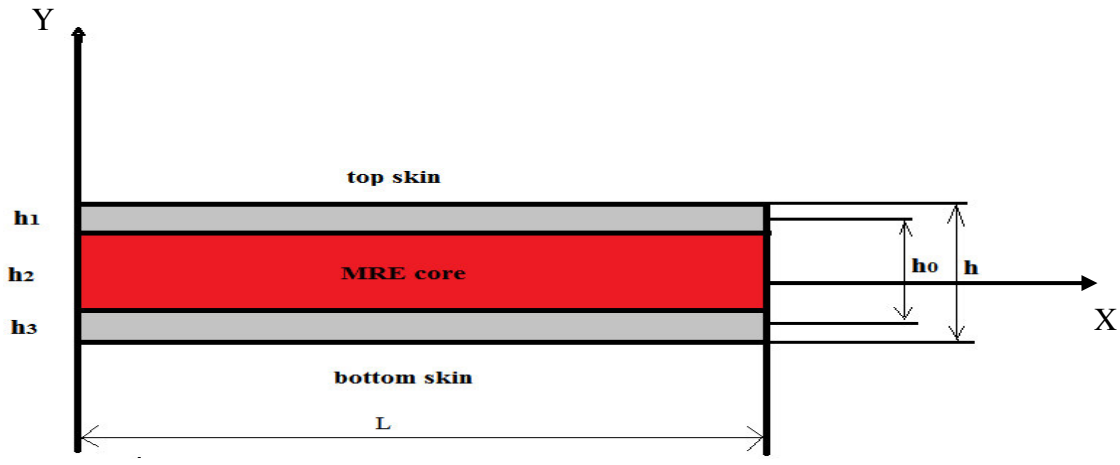

Figure II.1. magnetorheological sandwich beam model

II.2.1. displacement field

The assumed displacement fields in the sandwich beam follows,

The longitudinal and transverse displacement fields for the top and bottom layer are given by:

$$u_i(x,z,t) = u_i(x,t) - z_i \frac{\partial w_i^0}{\partial x}(x,t) \tag{II.1}$$

$$w_i(x,z,t) = w_i^0(x,t) \tag{II.2}$$

where, u_i in the top and bottom layer for any (x, z) location, u_i^0 longitudinal displacement at the centroid of the top layer, z_i distance from centroid of top layer in transverse direction, w_i transverse displacement in the top layer for any (x, z) location, w_i^0 transverse displacement at the centroid of the top and bottom layer and (i =1, 3) is the local coordinate of the top and bottom layer.

Displacements field in the viscoelastic core layer varies nonlinearly in both x and z directions. By taking an elastic analysis, Bai and Sun [12] assumed that the longitudinal and transverse displacement of the core is

$$u_2(x,z_2,t) = u_2^0(x,t) + z_2\left(e\alpha(x,t) - \frac{\partial w_2^0(x,t)}{\partial x}\right) - \frac{z_2^2 \partial\beta(x,t)}{\partial x} + \frac{z_2^3 \partial^2\alpha(x,t)}{\partial x^2} \tag{II.3}$$

$$w_2(x,z_2,t) = w_2^0(x,t) + z_2\beta(x,t) - \frac{z_2^2}{2}\frac{\partial\alpha(x,t)}{\partial x} \tag{II.4}$$

$$e = 2(1+v_c) \tag{II.5}$$

Where u_2 longitudinal displacement in the MRE core layer for any (x, z) location u_2^0 longitudinal displacement at the centroid of the MRE core layer, z_2 distance from centroid of core layer in transverse direction, α shear deformation in MER core, β transverse normal deformation in MER core, w_2 transverse displacement in core layer for any (x, z) location, w_2^0 transverse displacement at the centroid of the MER core layer and v_c poisson's ratio of viscoelastic core layer.

To describe the displacement field for the core layer, four generalized degrees of freedom u_2^0, w_2^0 and β are required. Non linear displacement field of a viscoelastic core layer allows the transverse displacement of top constrained layer and bottom layer to remain independent of each other. This leads to transversal extension and compression of the core layer. As assumed

in the assumptions that there is the perfect bond between the three layers the following relation are used:

At top interface

$$u_2\left(x,h_2/2,t\right)=u_1\left(x,-h_1/2,t\right) \tag{II.6}$$

$$w_2\left(x,h_2/2,t\right)=w_1\left(x,-h_1/2,t\right) \tag{II.7}$$

At bottom interface,

$$u_2\left(x,h_2/2,t\right)=u_3\left(x,-h_3/2,t\right) \tag{II.8}$$

$$w_2\left(x,h_2/2,t\right)=w_3\left(x,-h_3/2,t\right) \tag{II.9}$$

Now substituting the displacement fields of the MRE core layer from Eq. (3) and Eq. (4) into Eq. (6), (7), and (8), (9), out of four degrees of freedom it is possible to eliminate the three degrees of freedom in core layer, specifically through the following relations

$$u_2^0=\frac{1}{2}\left[u_1^0+u_3^0-\left(\frac{h_1}{2}+\frac{h_2}{4}\right)\frac{dw_1^0}{dx}-\left(\frac{h_3}{2}+\frac{h_2}{4}\right)\frac{dw_3^0}{dx}\right] \tag{II.10}$$

$$w_2^0=\frac{w_1^0+w_3^0}{2}+\frac{h_2^2}{8}\frac{\partial\alpha}{\partial x} \tag{II.11}$$

$$\beta=\frac{w_1^0-w_3^0}{2} \tag{II.12}$$

II.2.2. Mathematical model

The bar OH is a length » L », built in O is subjected to the linear density of the force P (x)

And the force F_x in A

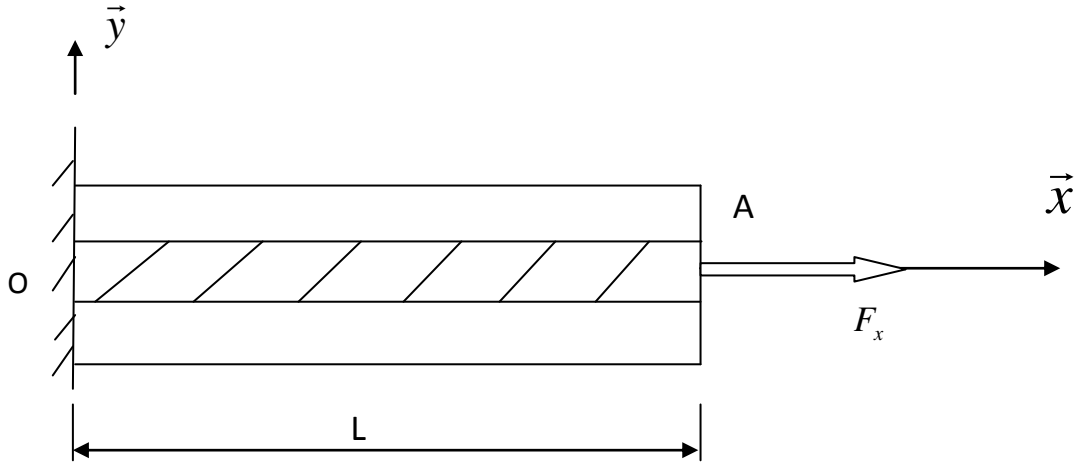

Figure.II.2. Traction bar diagram

II.2.3. Theorem of virtual works

The Theorem of virtual works is written:

$$\int_0^L ES\frac{du}{dx}\frac{d\delta u}{dx}dx - F\delta u(L) - \int_0^L p(x)\delta u(x)dx = 0 \qquad \text{(II.13)}$$

Or: $u(x)/u(0) = 0$ Checked the relationship $\forall \delta u(x)/\delta u(0) = 0$

By introducing the displacement

$$u(x) = c_j \varphi_j(x_1) \text{ With } \varphi_j(0) = 0 \text{ , } j = 1,2,...,n. \qquad \text{(II.14)}$$

And the displacement virtual:

$$\delta u(x_i) = \delta c_i \varphi_i(x_1), \ i = 1,2,...,n. \qquad \text{(II.15)}$$

In the expression of the theorem of the virtual works, on obtains:

$$\int_0^L ES\, c_j \frac{d\varphi_j}{dx_1}\frac{d\varphi_i}{dx}dx_1 - F\delta C_i \varphi_i(L) - \int_0^L p(x_1)\delta c_i \varphi_i(x)dx_i = 0, \forall \delta C_i \qquad \text{(II.16)}$$

We still again:

$$(a_{ij}c_j - b_i)\delta C_i = 0, \forall \delta C_i, with \quad a_{ij} = a_{ji} = \int_0^L ES \frac{d\varphi_i}{dx_1}\frac{d\varphi_j}{dx_1} dx_1 \tag{II.17}$$

$$b_i = F\varphi_i(L) + \int_0^L p(x_1)\varphi_i(x_1)dx_1 \tag{II.18}$$

The variational formulation thus obtained is verified whatever scissile n constants C_j are solutions of the algebraic system:

$a_{ij}c_j = b_i$

II.2.4. Theorem of potential energy

The potential energy in this case is given as follows:

$$E_p = \int_0^l ES(\frac{du}{dx_1})^2 dx_1 - Fu(L) - \int_0^L p(x_1)u(x_1)dx_1 \tag{II.19}$$

Is minimized if:

$$\delta E_p = \frac{\partial E_p}{\partial C_i}\delta C_i = 0 \tag{II.20}$$

The values of n constants c_j which minimize the potential energy cancel the "n" partial derivatives $\partial Ep / \partial c_i = 0$, which are equal to:

$$\frac{\partial E_p}{\partial c_i} = \int_0^l ES \frac{du}{dx_1}\frac{\partial}{\partial c_i}(\frac{du}{dx_1})\ dx_1 - F\frac{\partial u}{\partial c_i}u(L) - \int_0^L p(x_1)\frac{\partial}{\partial c_i}[u(x_1)]dx_1 \tag{II.21}$$

whether:

$$\frac{\partial E_p}{\partial c_i} = \int_0^l ESC_i \frac{d\varphi_j}{dx_1}\frac{d\varphi_i}{dx_1} dx_1 - F\varphi_i(L) - \int_0^L p(x_1)\varphi_i(x_1)dx_1 = 0 \tag{II.22}$$

N finds the system $a_{ij}c_j = b_j$ which was obtained from the virtual works theorem.

II.3. Numerical modeling

The structure studied in the work is considered as a bar of languor L Discretized into six elements. The recessed bar at L, is subjected to the action of gravity and the force Fx, where x Is vertical descending, Applied to the surface center of The non-recessed terminal section

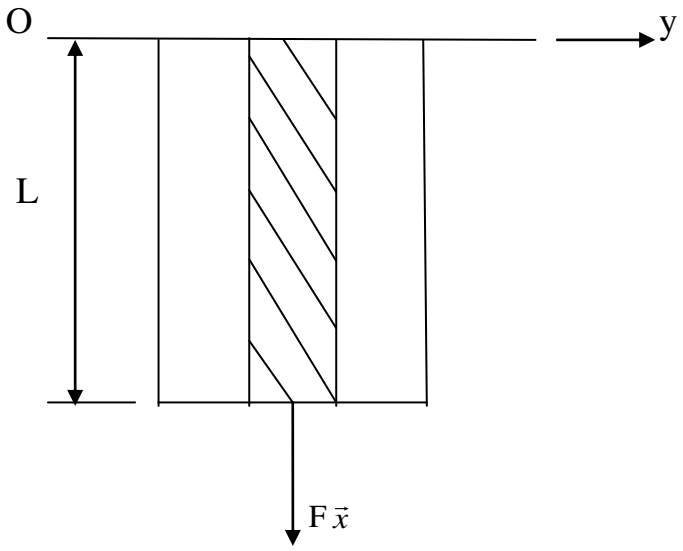

Figure. II.3. Vertical bar with traction

The six basic functions considered are given by:

$$\varphi_i(x) = (\frac{x}{L})^i, i = 1,...,6. \quad \text{(II.23)}$$

The displacement, u(x) depends on six entries, C_i, 1,6 which check system of equations:

$$a_{ij} c_j = b_i$$

Where:

$$U_i^n = \sum_{i=1}^{n} C_i (\frac{x}{l})^i = \sum_{i=1}^{n} C_i \varphi_i(x) \quad \text{(II.24)}$$

The n constants C_i are calculated by:

$$C_i = K_{ij} F_j \quad \text{with} \quad \begin{matrix} i = 1,n \\ j = 1,n \end{matrix} \quad \text{(II.25)}$$

II.3.1. Ritz method

In the Ritz method, the shape of deformation of the continuous system is approximated using a series of trial shape functions the must satisfy of the continuous system can be written as

$$u(x) = C_1\varphi_1(x) + C_2\varphi_2(x) + ... + C_n\varphi_n(x) = \sum_{j=1}^{n} C_j \varphi_j(x) \quad \text{(II.26)}$$

Where φ_1, φ_2, ... and φ_n are trial shape functions which can be the Eugen functions, a set of assumed mode shapes, or a set of polynomials, and C_1, C_2, ... C_n are constant coefficient called the Ritz coefficients.

In Eq. (II.26), the functions $\varphi_1, \varphi_2 ... \varphi_n$ are assumed to be known, while the coefficients C_1, C_2 ..., and C_n are adjusted by minimizing the Rayleigh equation with respect to each of these coefficients. The procedure leads to a homageneaus system of n algebraic equations the matrix mass and stiffness matrix coefficients are determined by

$$m_{ij} = \int_0^l lA\,\varphi_i \varphi_j dx \tag{II.27}$$

$$K_{ij} = \int_0^l EA\,\varphi_i \varphi_j dx \tag{II.28}$$

Calculation of element of the "stiffness matrix"

$$K_{11} = E_q S \int_0^L \left(\left(\frac{d}{dx}\left(\frac{x}{L} \right) \right)^2 \right) dx = \frac{E_q S}{L} \tag{II.29}$$

$$K_{22} = E_q S \int_0^L \left(\left(\frac{d}{dx}\left(\frac{x}{L} \right)^2 \right)^2 \right) dx = \frac{4}{3}\frac{E_q S}{L} \tag{II.30}$$

$$K_{33} = E_q S \int_0^L \left(\left(\frac{d}{dx}\left(\frac{x}{L} \right)^3 \right)^2 \right) dx = \frac{9}{5}\frac{E_q S}{L} \tag{II.31}$$

$$K_{44} = E_q S \int_0^L \left(\left(\frac{d}{dx}\left(\frac{x}{L} \right)^4 \right)^2 \right) dx = \frac{16}{7}\frac{E_q S}{L} \tag{II.32}$$

$$K_{55} = E_q S \int_0^L \left(\left(\frac{d}{dx}\left(\frac{x}{L} \right)^5 \right)^2 \right) dx = \frac{25}{9}\frac{E_q S}{L} \tag{II.33}$$

$$K_{66} = E_q S \int_0^L \left(\left(\frac{d}{dx}\left(\frac{x}{L} \right)^6 \right)^2 \right) dx = \frac{36}{11}\frac{E_q S}{L} \tag{II.34}$$

$$K_{12} = E_q S \int_0^L \frac{d}{dx}\left(\frac{x}{L}\right) dx . \int_0^L \frac{d}{dx}\left(\frac{d}{L}\right)^2 dx = \frac{E_q S}{L} \tag{II.35}$$

$$K_{13} = E_q S \int_0^L \frac{d}{dx}\left(\frac{x}{L}\right) dx . \int_0^L \frac{d}{dx}\left(\frac{d}{L}\right)^3 dx = \frac{E_q S}{L} \tag{II.36}$$

$$K_{14} = E_q S \int_0^L \frac{d}{dx}\left(\frac{x}{L}\right) dx . \int_0^L \frac{d}{dx}\left(\frac{d}{L}\right)^4 dx = \frac{E_q S}{L} \tag{II.37}$$

$$K_{15} = E_q S \int_0^L \frac{d}{dx}\left(\frac{x}{L}\right) dx . \int_0^L \frac{d}{dx}\left(\frac{d}{L}\right)^5 dx = \frac{E_q S}{L} \tag{II.38}$$

$$K_{16} = E_q S \int_0^L \frac{d}{dx}\left(\frac{x}{L}\right) dx . \int_0^L \frac{d}{dx}\left(\frac{d}{L}\right)^6 dx = \frac{E_q S}{L} \tag{II.39}$$

$$K_{23} = E_q S \int_0^L \frac{d}{dx}\left(\frac{x}{L}\right)^2 dx . \int_0^L \frac{d}{dx}\left(\frac{d}{L}\right)^3 dx = \frac{3}{2}\frac{E_q S}{L} \tag{II.40}$$

$$K_{24} = E_q S \int_0^L \frac{d}{dx}\left(\frac{x}{L}\right)^2 dx . \int_0^L \frac{d}{dx}\left(\frac{d}{L}\right)^4 dx = \frac{8}{5}\frac{E_q S}{L} \tag{II.41}$$

$$K_{25} = E_q S \int_0^L \frac{d}{dx}\left(\frac{x}{L}\right)^2 dx . \int_0^L \frac{d}{dx}\left(\frac{d}{L}\right)^5 dx = \frac{5}{3}\frac{E_q S}{L} \tag{II.42}$$

$$K_{26} = E_q S \int_0^L \frac{d}{dx}\left(\frac{x}{L}\right)^2 dx . \int_0^L \frac{d}{dx}\left(\frac{d}{L}\right)^6 dx = \frac{12}{7}\frac{E_q S}{L} \tag{II.43}$$

$$K_{34} = E_q S \int_0^L \frac{d}{dx}\left(\frac{x}{L}\right)^3 dx . \int_0^L \frac{d}{dx}\left(\frac{d}{L}\right)^4 dx = \frac{2E_q S}{L} \tag{II.44}$$

$$K_{35} = E_q S \int_0^L \frac{d}{dx}\left(\frac{x}{L}\right)^3 dx . \int_0^L \frac{d}{dx}\left(\frac{d}{L}\right)^5 dx = \frac{15}{7}\frac{E_q S}{L} \tag{II.45}$$

$$K_{36} = E_q S \int_0^L \frac{d}{dx}\left(\frac{x}{L}\right)^3 dx . \int_0^L \frac{d}{dx}\left(\frac{d}{L}\right)^6 dx = \frac{9}{4}\frac{E_q S}{L} \tag{II.46}$$

$$K_{45} = E_q S \int_0^L \frac{d}{dx}\left(\frac{x}{L}\right)^4 dx . \int_0^L \frac{d}{dx}\left(\frac{d}{L}\right)^5 dx = \frac{5}{2}\frac{E_q S}{L} \tag{II.47}$$

$$K_{45} = E_q S \int_0^L \frac{d}{dx}\left(\frac{x}{L}\right)^4 dx . \int_0^L \frac{d}{dx}\left(\frac{d}{L}\right)^5 dx = \frac{5}{2}\frac{E_q S}{L} \tag{II.48}$$

$$K_{46} = E_q S \int_0^L \frac{d}{dx}\left(\frac{x}{L}\right)^4 dx . \int_0^L \frac{d}{dx}\left(\frac{d}{L}\right)^6 dx = \frac{8}{2}\frac{E_q S}{L} \tag{II.49}$$

$$K_{56} = E_q S \int_0^L \frac{d}{dx}\left(\frac{x}{L}\right)^5 dx . \int_0^L \frac{d}{dx}\left(\frac{d}{L}\right)^6 dx = \frac{3E_q S}{L} \tag{II.50}$$

Therefore, the stiffness matrix are given as follows

$$K = \frac{E_q S}{L}\begin{pmatrix} 1 & \frac{1}{4} & \frac{1}{3} & \frac{1}{8} & \frac{1}{5} & \frac{1}{12} \\ 1 & \frac{3}{2} & \frac{9}{5} & 2 & \frac{15}{7} & \frac{9}{4} \\ 1 & \frac{8}{5} & 2 & \frac{16}{7} & \frac{5}{2} & \frac{8}{5} \\ 1 & \frac{5}{3} & \frac{15}{7} & \frac{5}{2} & \frac{25}{9} & 3 \\ 1 & \frac{12}{7} & \frac{9}{4} & \frac{8}{3} & \frac{36}{11} & \frac{36}{11} \end{pmatrix} \tag{II.51}$$

The inverse stiffness matrix is given by relation (II.52) below.

$$K^{-1} = \frac{L}{E_q S}\begin{pmatrix} \frac{125112276}{8326145} & -\frac{83644155}{1665229} & \frac{84122080}{1665229} & -\frac{333270}{1665229} & -\frac{23984256}{1665229} & \frac{2414874}{8326145} \\ -\frac{451696203}{8326145} & \frac{403271715}{1665229} & -\frac{457702140}{1665229} & \frac{2998800}{1665229} & \frac{146407590}{1665229} & -\frac{23183622}{8326145} \\ \frac{117754112}{1665229} & -\frac{593100900}{1665229} & \frac{722158080}{1665229} & -\frac{7771400}{1665229} & -\frac{252564480}{1665229} & \frac{13524588}{1665229} \\ -\frac{51251130}{1665229} & \frac{277538940}{1665229} & -\frac{357151200}{1665229} & \frac{6652800}{1665229} & \frac{139669110}{1665229} & -\frac{15458520}{1665229} \\ \frac{2172744}{8326145} & -\frac{3620610}{1665229} & \frac{7237440}{1665229} & \frac{13230}{1665229} & -\frac{10153584}{1665229} & \frac{30444876}{8326145} \\ \frac{222418}{8326145} & -\frac{444990}{1665229} & \frac{1335740}{1665229} & -\frac{1560160}{1665229} & \frac{626220}{1665229} & -\frac{6468}{8326145} \end{pmatrix}$$

(II.52)

Calculation of the displacement coefficients

$$C_1 = \frac{1}{430602895}\frac{1}{ESL^5}(2816124570\rho gSL^2 + 43062895FL^6 - 29438926\rho gS - 71733816\rho gSL - 6097941640\rho gSL^3 + 3751036569L^4\rho gS + 62556138L^7\rho gS) \quad \text{(II.53)}$$

$$C_2 = -\frac{1}{1314818}\frac{\rho g}{EL^5}(11970504L^2 + 638505L^7 - 267060 + 11628190L^4 - 22865850L^3 - 446880L) \quad \text{(II.54)}$$

$$C_3 = \frac{140}{86120579}\frac{\rho g}{EL^5}(-947177L^4 + 300436L^7 - 132216L^2 - 78787 + 846608L^3 + 11136L) \quad \text{(III.55)}$$

$$C_4 = -\frac{35}{3744373}\frac{\rho g}{EL^5}(207L^7 - 67392L^2 + 14216 - 26040L^4 + 79450L^3 - 441L) \quad \text{(II.56)}$$

$$C_5 = \frac{2}{86120579}\frac{\rho g}{EL^5}(-9444141L^2 - 252030 + 285534L^7 - 7429555L^4 + 15169320L^3 + 1670872L) \quad \text{(II.57)}$$

$$C_6 = \frac{231}{430602895}\frac{\rho g}{EL^5}(-2804 + 5227L^7 - 3004120L^2 - 766074L^4 + 2639315L^3 + 1128456L) \quad \text{(II.58)}$$

$$C_1 = \frac{1}{ESL^5}(6.5399\rho gSL^2 + 0.1FL^6 - 0.0684\rho gS - 0.1666\rho gSL - 14.1614\rho gSL^3 + 8.7111\rho gSL^4 + 0.1453\rho gSL^7) \quad \text{(II.59)}$$

$$C_2 = \frac{1}{ESL^5}(\rho g S(9.1043L^2 + 0.4856L^7 - 0.2031 + 8.8439L^4 + 17.3909L^3 - 03399L)) \quad \text{(II.60)}$$

$$C_3 = \frac{\rho g}{EL^5}(-1.5397L^4 + 0.4884L^7 - 0.2149L^2 - 0.1281 + 1.3763L^3 + 0.0181L) \quad \text{(II.61)}$$

$$C_4 = \frac{\rho g}{EL^5}(0.0019L^7 - 0.6299L^2 + 0.1329 - 0.2434L^4 + 0.7426L^3 - 0.0041L) \quad \text{(II.62)}$$

$$C_5 = \frac{\rho g}{EL^5}(-4.6058L^2 - 0.1229 + 0.1392L^7 - 3.6233L^4 - 7.3979L^3 + 0.8149L) \quad \text{(II.63)}$$

$$C_6 = \frac{\rho g}{EL^5}(-0.0015 + 0.0028L^7 - 1.6116L^2 - 0.4109L^4 + 1.4159L^3 + 0.6054L) \quad \text{(II.64)}$$

II.4. Conclusion

In this chapter, are presented of the theories performed to allow describing the behavior of the beams and the energy methods, these latest exposed methods in this chapter have been used for the analytical modelisations digital and the beam magnetorheologique which will be presented in the next chapter.

CHAPTER II

Static analysis of beam with magnetorheological elastomer core

III.1. Introduction

The present work is devoted to the experimental analysis of the behavior of the composite in Mgnetorheogical elastomers under dynamic loading. The development of the elastomer charged to 40% ferromagnetic particles, the characterization of the rheological properties and the interaction between the loads as a function of the magnetic field have been studied. The results found shows that this composite presents strong energy dissipation, further accentuated by the structuring and the magnetic field.

III. 2. Brief overview on the modeling of MRE

during dynamic solicitations, An elastomer exhibits a viscoelastic behavior, That is to say that it presents at the same time the properties of a elastic solid, and also those of a viscous fluid .[13,14] The composite structured can even goes further, because the viscoelastic properties can be controlled by the intermediate of a magnetic field [15,16]. The issue here is to understand the significant energy dissipation of the structured composite, which increased in the presence of a field [17]. The 80's saw the birth of an interest for the materials with variables properties under the influence of an external factor; the temperature, the electric or magnetic fields. Included in their ranks the Mgnetorheogical elastomers (MRE)[18]. These materials (MRE) are composed of magnetic particles polarizable dispersed in a matrix, generally made from silicone oil. Today much of scientific laboratories conduct research on the MRE. Usually elastomers for flexible silicone or polyurethane are used for polymer matrix they are filled with a significant share of magnetic particles, Often 30% of the volume. To reduce the amount of magnetic particles, a vulcanization process forced by a magnetic field has been used in order to increase their efficiency. The MRE mad of soft facts matrices of silicone or polyurethane show a response to magnetic fields significant but their low mechanical properties prevent them to be used in engineering [19]. It is expected that these materials, although they are in the development phase, Will be very useful for solving problems of vibrations, which are recurring problems for the construction and the use of machines or systems. The Mgnetorheogical effect and properties of damping are fundamental for the applications of MRE. They are used in particular to achieve the dampers, the bushings of suspensions to variable stiffness and magnetostrictive materials [20]. For MRE it is agreed the magnetic phenomenon which matters. To determine the magnetic parametres, it is necessary to design the test bench beforehand and to prepare the test to obtain the desired

characteristics. In order to obtain the curve of magnetic hysteresis of the MRE, the tools and following experiments were accomplished [21], [22] In these last years, The scientific community is concentrated on the knowledge of the rheological behavior. Valery P and al [23] have studied the isolation from vibrations by the use of Mgnetorheogical elastomers. This experimental work mainly presents the parameters the most important of the active shock absorber. Mirosław Bocian and al [24] elaborate a mechanical structure based on a Mgnetorheogical elastomer, This elastomer has been designed for the absorbation of energy and the mitigation of the vibratory movements from a excitation of impact. A mathematical model adequate to been derived by Mateusz Kukla and al [25], this work presents the results of the analysis of the behavior in compression and the effect of the static magnetic field on the latter. It also presents attempts to use of rheological models to describe the MRE. The influence of radiation on the module of shearing of the Mgnetorheogical elastomers was studied [26]. The experimental results show that the initial shear modulus and the magnetic field shear modulus induced as increases in the first, and then decrease with the increase of the radiation dose. Two factors are considered for explaining the experimental results. One is the reaction of crosslinking and degradation induced by radiation, the other is the change of the magnetization of the saturation of the particle of iron carbonyl.

In this work we have studied the influence of the variable magnetic field on the rheological properties of an elastomer loaded in 40% of iron particles. First of all the development of the sample of Mgnetorheogical elastomers is presented. Then the influence of the magnetic field on the dynamic properties adjustable from the sample of MRE is studied experimentally using Viscoanalyseur dynamics and results obtained for different intensities of the magnetic field are presented.

III.3. Theoretical modeling

In this work, we will see that the model of generalized Maxwell is suitable for describing the mechanical behavior of our elastomer, this model consists of the spring and N models of Maxwell assembled in parallel (figure.III.1). The modules of elasticity are denoted by $G_0, G_1, G_2, \ldots, G_n$ While viscosity coefficients are designated by η_1, $\eta_2, \ldots, \eta_n$.

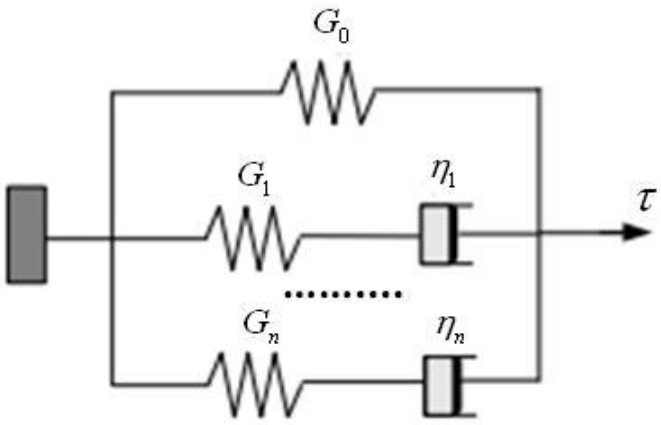

Figure.III.1. Model of generalized Maxwell

III.4. Laminated functionally graded beam with interlayer

Considering two functionally graded layers bonded by viscoelastic elastomer witch can be modeled by Maxwell-wiechert model. This model contains a series of spring-dashpot units and hookean spring. The time-depandent shear modulus G(t) of the viscoelastic elastomer decays with time and can be expressed as prony series:

$$G(t) = G_\infty + \sum_{i=1}^{N} G_i e^{-t/\tau_i} \tag{III.1}$$

Where G_i, G_∞ and τ_i are the long-term shear modulus, the relaxation shear moduli and the relaxation time.

The deformation of the model is the sum of the deformations of the two elements, Reversible represented by the spring element and viscous corresponding to the damper such as:

$$\tau = E\varepsilon + \gamma\dot{\varepsilon} \tag{III.2}$$

Based on boltzman superposition principle, the shear stress $\tau(x,t)$ can be expressed as:

$$\tau(x,t) = G(t)\gamma(x,0) + \int_0^t G(t-\xi)\frac{\partial\gamma(x,\xi)}{\partial\xi}d\xi = G(t)^* d\gamma(x,t) = \gamma(x,t)^* dG(t) \tag{III.3}$$

Where the (*) denotes convolution. The equation above describes relaxation constitutive relationship. After fourier transform, can be expressed as:

$$\tau(x,\omega) = i\omega G(\omega).\gamma(x,\omega) \tag{III.4}$$

Where $G(\omega)$ is the Fourier transform of shear modulus $G(t)$ and i denotes $\sqrt{-1}$, can also be written as:

$$\tau(x,\omega) = G^*(\omega).\gamma(x,\omega) \quad \text{(III.5)}$$

To take account of the duality between viscosity and elasticity, It frequently uses complex numbers (two components) when a material is subjected to a dynamic solicitation, the complex module $G^*(t)$ for a solicitation in shear, writes:

$$G^* = G' + iG'' = G'(1 + i\eta) \quad \text{(III.6)}$$

G', The real part, called a module of conservation, that characterizes the rigidity of the elastomer and G'' the imaginary part, called a module of dissipation, which characterizes the viscous behavior.

The loss factor or damping factor is written:

$$\tan(\delta) = \frac{G''}{G'} = \eta \quad \text{(III.7)}$$

III.4.1. Material and experimental analysis

III.4.1.1. MRE material and implementation

The elaborated composite is an elastomer of silicone oil, RTV 141 and RTV 141B associated with ferromagnetic loads of average diameter 1.8-2.3 μm. The powder is carefully mixed with elastomer, first by hand (Figure.III.2.a) and then in a mixer for 1 hour to break the maximum aggregates and homogenize the mixture. The latter is degassed under vacuum for 15 minutes and then poured into a rectangular shaped mold with two coils (Figure.III.2.b), The mixture is then moved into sliding movement to prevent sedimentation of the particles during crosslinking under a magnetic field. The time of cross-linking is very sensitive to both the temperature and to the nature of the particles The silicone oil composite, RTV 141 and iron particles are cross-linking in 24 h at ambient temperature of 27°C. The rheological properties are determined using a Viscoanalyseur DMT450 of laboratory (LPMC) (Figure.III.2). And at a constant frequency of 50 Hz

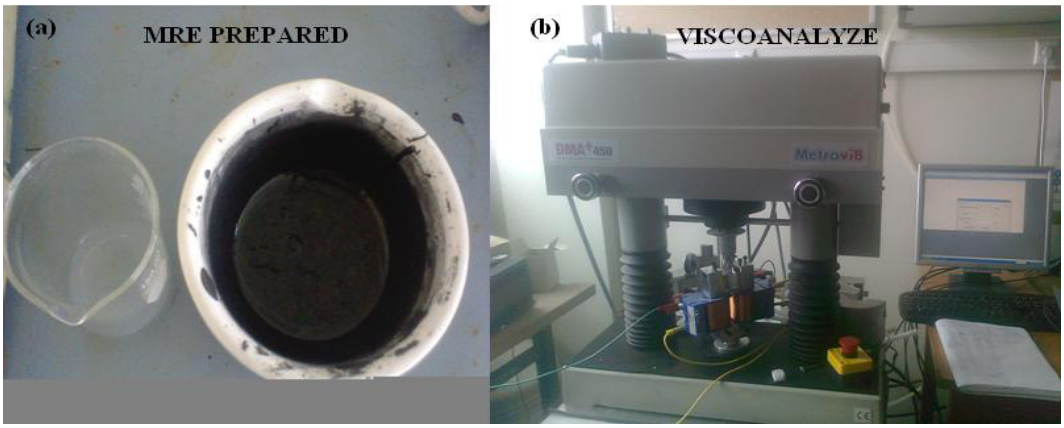

Figure.III.2. a) Prepared Elastomer, b) Dynamic viscoanalyseur **DMA^{+}450**

The ingredients of a rectangular magnetorheological elastomer specimen of 35 mm length, 25 mm width and 2 mm thickness loaded with 40% iron particles of its total volume. are given in Table 1.

Table1. Constituents of the Mgnetorheogical elastomers

Loaded elastomer to 40% ferromagnetic particles				
Time of reticulationen Hours	$m_{Silicon\ Oil}$ (g)	$m_{RTV(A)}$ (g)	m_{Fe} (g)	$m_{RTV(B)}$ (g)
24h	1.064g	1.0385g	7.559	0.104

III.5. Results and Discussion

The modules-deformation curves of isotropic composites loaded to 40% with and without magnetic field are compared (Figure.3.a,b). in this figure, We observe that the pace of the curves of the conservative and dissipative module decreases as a function of the increase in shear deformation, we distinguish a sudden change of the conservative and dissipative modules for a shear deformation of less than 4%, then a Slow variation for shear deformation greater than 4%

The explanation of this stiffening of the material submitted to a field is the following: at the microscopic level, the magnetic field creates attractive interparticle force whose the consequence is to strongly stiffen the chains of particles, which then act as real small fibers.

Then, during the deformation, the elastic stress will exceed the magnetic stress and the fibers will be progressively broken into ever shorter elements

On the other hand there is a significant increase in these modules is observed under the influence of the magnetic field.

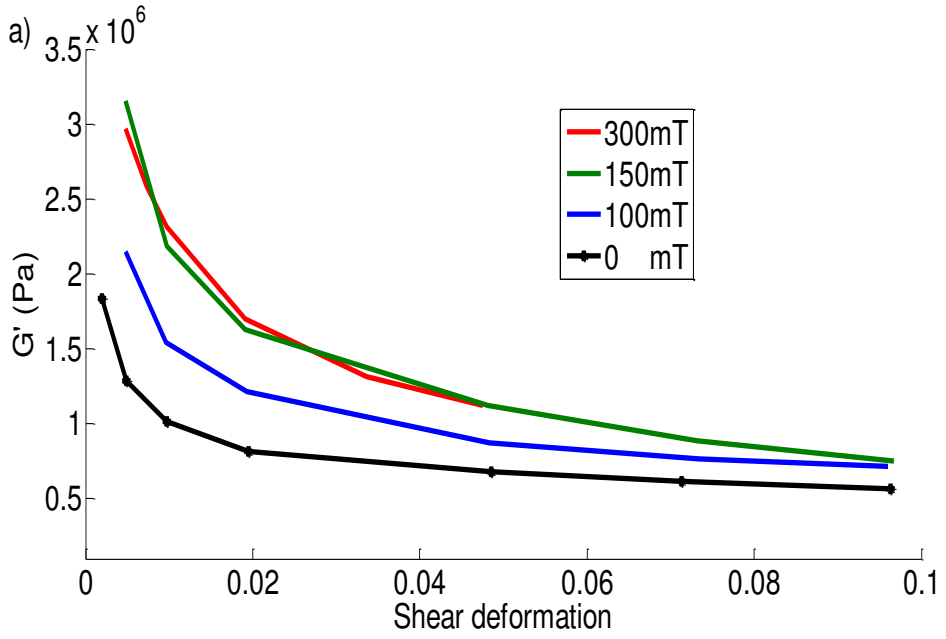

Figure.III.3.a. Comparesent between consirvation modul and shear deformation by different values (mT)

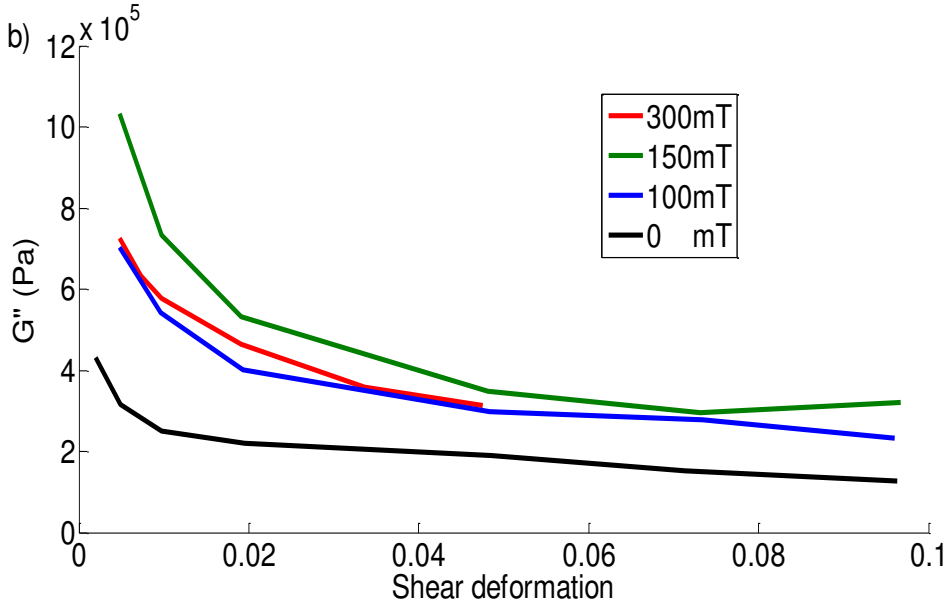

Figure.III.3.b. Comparesent between dissipation modul and shear deformation by different values (mT)

The Figure.III.4 shows the evolution of the angle of loss a function of shear deformation, as shown in this figure, the magnetic field plays an important role in the energy dissipation, we observe that the loss factor increases very strongly with the increase of the magnetic field. On the other hand, the angle of loss shows clear differences (Fig. 4): the fraction of energy dissipated increases with the field and with the creation of the pseudo-fibers formed by the ferromagnetic particles

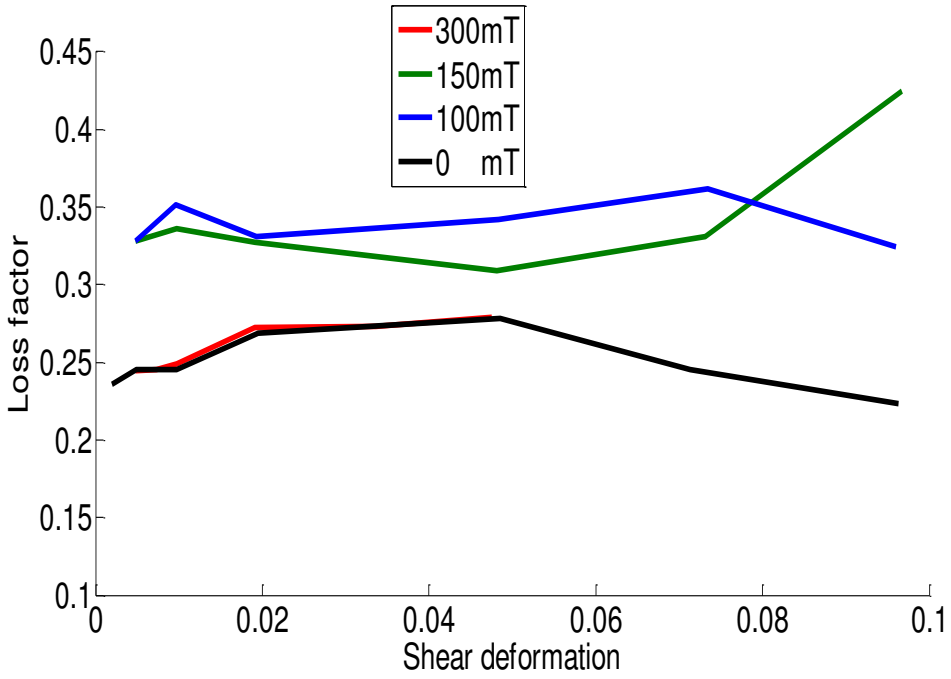

Figure.III.4. Variation of loss factor a function of shear deformation by different values of magnetic field.

The results of quasi-static tests are illustrated in (Figure.III.5), a strong effect Mgnetorheogical is observed on our composite loaded to 40%, Sign of an interaction between chains. It should be noted that the magnetic field considerably modifies the rheological properties and plays essentially on the shear deformation.In addition, the decrease and the relative increase of G' is a little intense than for the dissipative module G'' or the addition of oil strongly reduces the local constraints and requires stronger deformations to access critical constraints.

The magnetic field despite all small defects (bad aggregates, bad alignments of chains, columns of particles very close ...), which then contribute to the interaction between

neighboring chains and during solicitations, we will be as many additional detachments, Which are reflected at the microscopic level by the accentuated G' and G''.

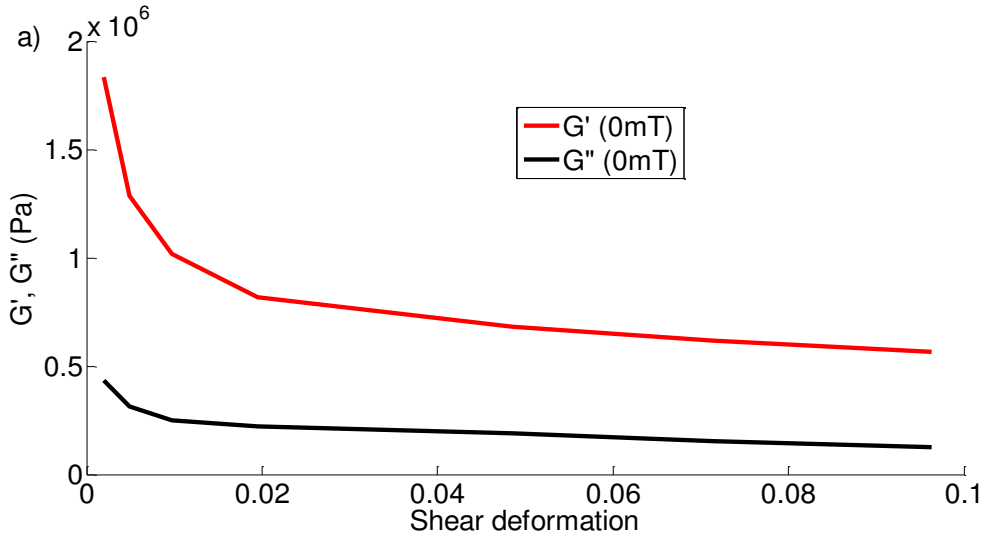

Figure.III.5.a. Difference between consirvation and dissipation a fonction of shear deformation withe (0 mT)

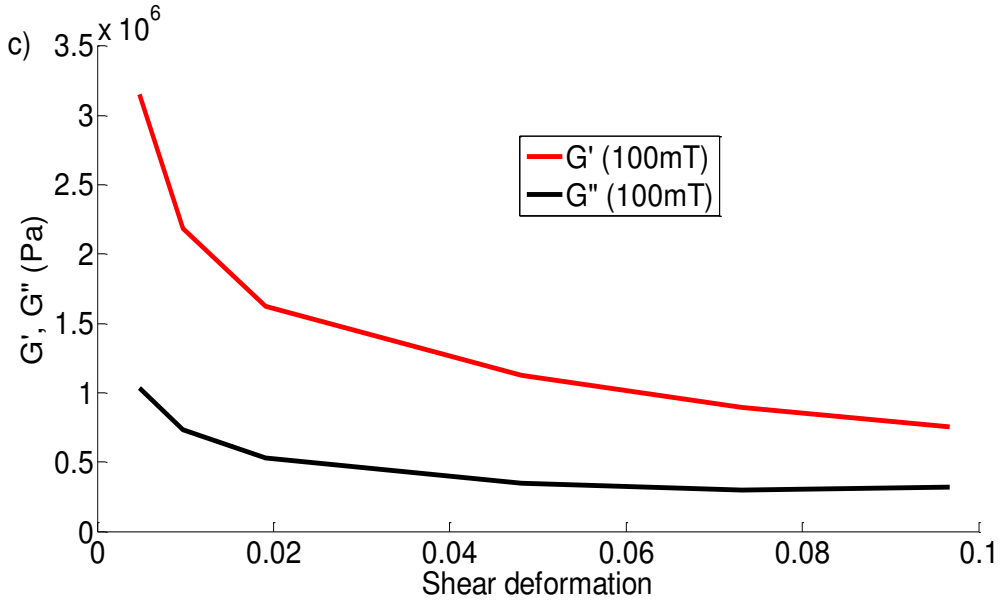

Figure.III.5.b. Difference between consirvation and dissipation a fonction of shear deformation withe (100 mT)

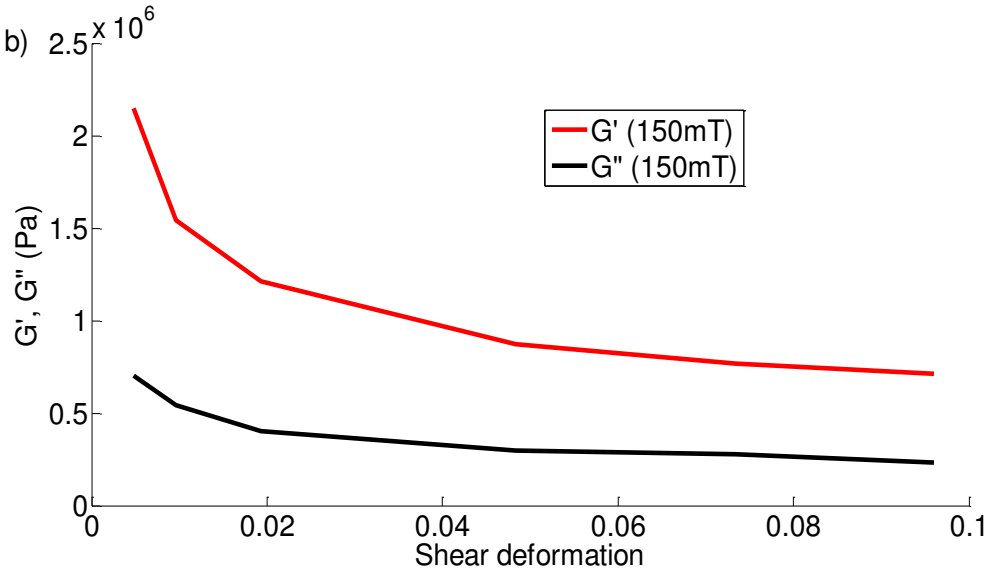

Figure.III.5.c. Difference between consirvation and dissipation a fonction of shear deformation withe (150 mT)

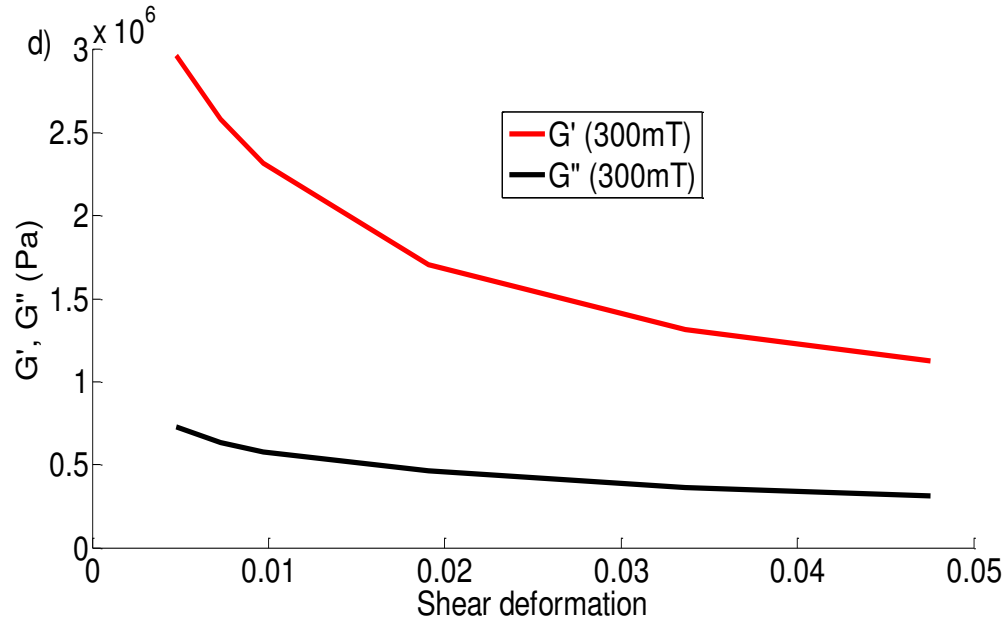

Figure.III.5.d. Difference between consirvation and dissipation a fonction of shear deformation withe (300 mT)

III.6. Conclusions

The magnetorheological elastomer loaded with 40% of iron particles is prepared under different magnetic fields. The microstructures are greatly affected by the magnetic flux,

density during the preparation. The MRE viscoelastic properties are also tested by a mechanical–magnetic coupling dynamic mechanical analyzer (DMA). The results show that the field-dependence of MRE viscoelastic properties increase with the applied magnetic flux densities during testing, the rheological properties of the elastomer also depend on the arrangement of their particles. The application of magnetic field leads to an important increase in elastic modulus. The results show a non-linear change in the rheological properties with respect to the variation of the magnetic field strength, it is due to the magneto-rheological effect.

CHAPTER III

Experimental study of composite sandwich beam

IV.1. Introduction

In this chapter we had simulate structures sandwich beam in case statics, we had simulated the sandwich beam which is consisted of three elements; two elastic skins. the bottom face sheet and the top face sheet and the third element is a soft core as like the sandwich beam in the real experience .to simulate and study the properties dynamic of this structures; we had used ABAQUS software which can give distribution of the stress, strain and field of the displacement and the deformation of the specimen. We had analyses three different cases of support, then finding diagrams variation of the forces (N) function of the elongation (mm) in a magnetic field for the three tests, then we compare With diagrams of Rayleigh Ritz method Which we have calculated

IV.2 Introduction of ABAQUS

ABAQUS is a compressive general purpose finite element program that contain 100.000 lines of code it is capable of performing static, dynamic, heat transfer, fluid flow an electromagnetism analysis, ABAQUS has a complete new look with a multiple window incorporating graphical user interface (GUI), pull down menus, dialog boxes and tool bar, Today we fined ABAQUS in the whole engineering field

IV.3. Structure

IV.3.1. description of the structure

Is the sandwich beam consists form three parts: the vescoelastic core in the middle which is made of elastomer and two elastic layers the bottom face sheet and the top face sheet which are mad of aluminum.

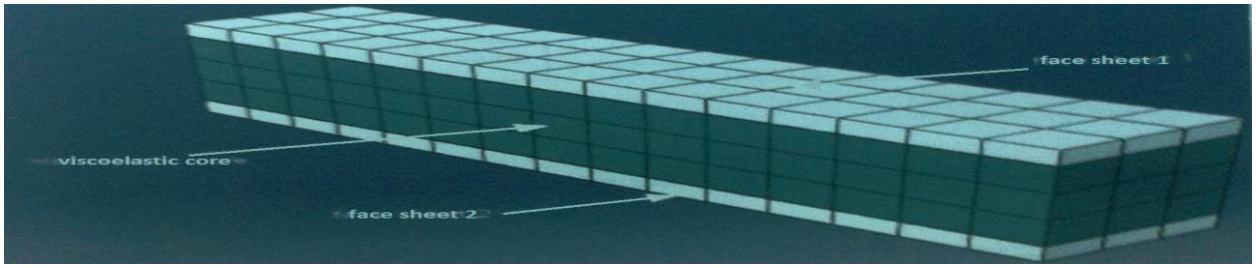

Figure.IV.1. the structure of the sandwich beam

IV.3.2. Geometrical parameters of the structure

The sandwich beam consists of elastomer and aluminum whose dimensions are provided in this table.

Table.IV.1. geometrical parameters of the sandwich beam

dimensions	Lenghth (mm)	Width (mm)	Thichness (mm)
Face sheet 1 Aluminum	35 mm	25 mm	1 mm
Viscoelastic Material elastomer	35 mm	25 mm	2 mm
Face sheet 2 Aluminum	35 mm	25 mm	1 mm

IV.3.3. Simulation in based to following steps

The simulation is based to following steps:

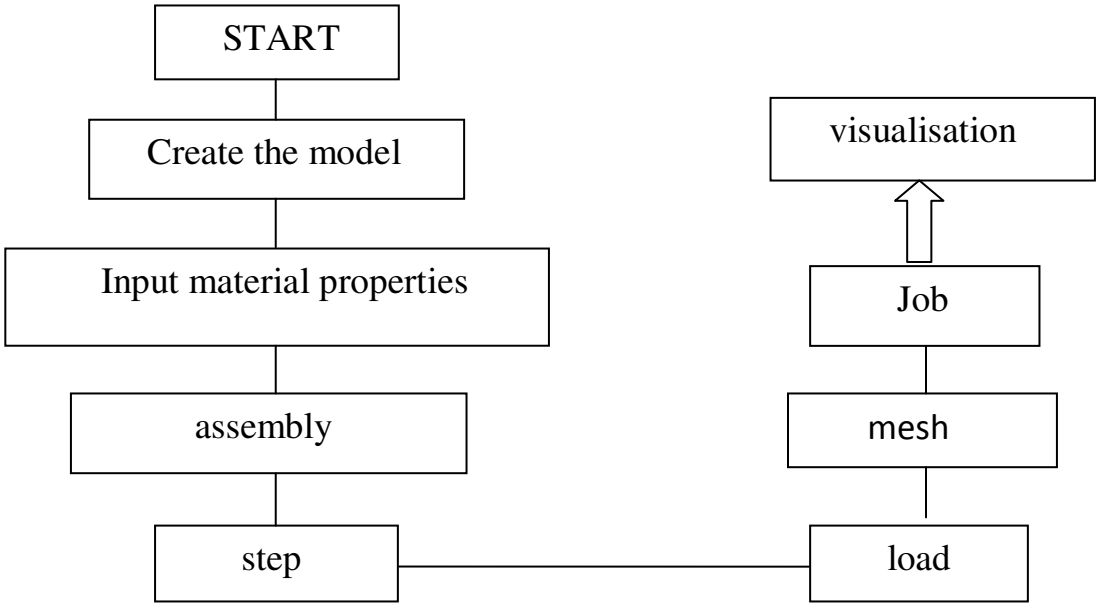

IV.3.3.1. Created model

The first step to create the structure is create the segments by drawing the vescoelastic core with its dimention, and then we draw the two face sheets with their dimension

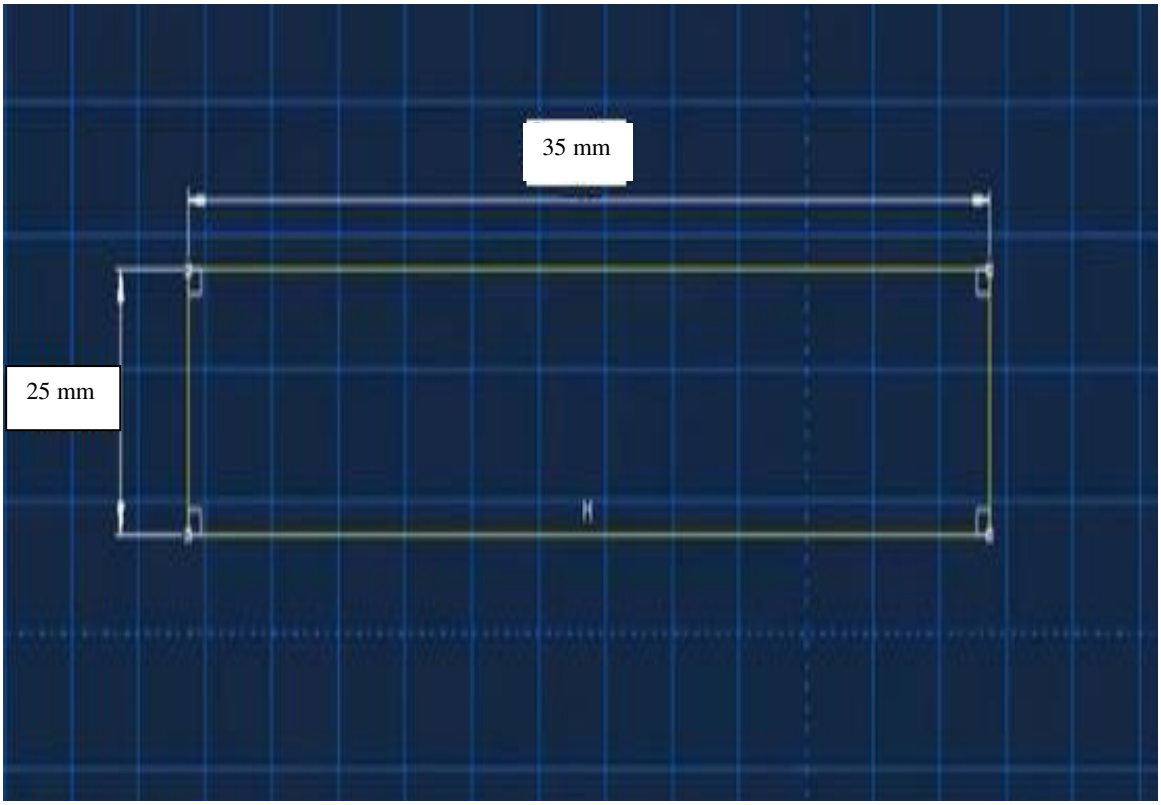

Figure.IV.2. The dimension of the layer in 2D

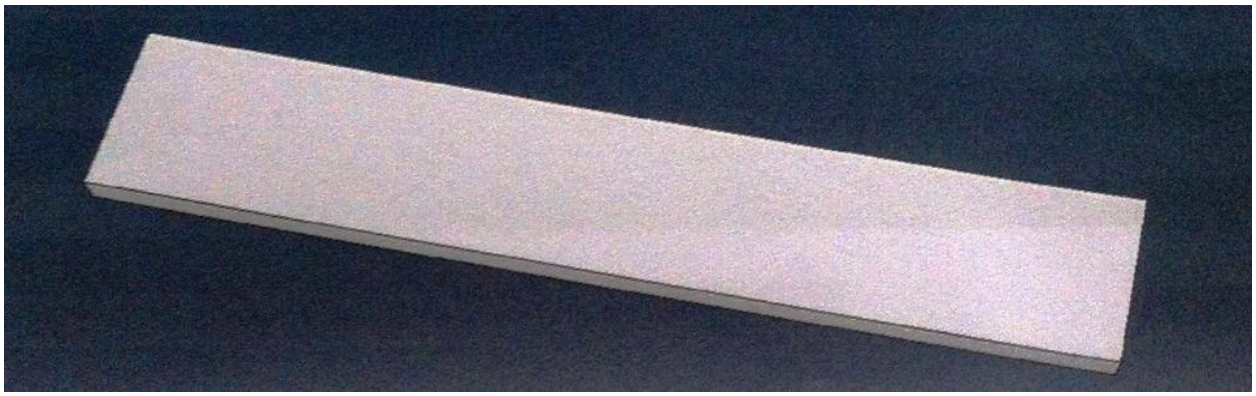

Figure.IV.3. The shapes of the two face sheet and the core in 3D

IV.3.3.2. properties of materials

After the creation the model we have to enter the material properties of the part to define the specimen properties of each material as shown in this table.

Table.IV.2. mechanical properties of sandwich beam

Material Type	Elastic modulus (E) [Mpa]	Density (ρ) [$^{Kg}/_{m^3}$]	Poisson's Ration (ϑ)
Face sheet 1 Aluminum	7200	7200	0.33
Viscoelastic Material elastomer	1.7	1100	0.44
Face sheet 2 Aluminum	7200	2700	0.33

Table.IV.3. rheological properties of the elastomer

Experimental properties of the elastomer magnetorheological		
Magnetic field	G' (Mpa)	G''(Mpa)
B= 0 T	1.6	0.33
B= 0.3 T	1.93	0.54
B= 0.5 T	2.07	0.35

IV.3.3.3. Assembly

Use the ABAQUS/CAE assembly module to create instances of our past and to contract an assembly by positioning those instances relative to each other in a global coordinate system and we can create our structure sandwich beam

Figure.IV.4. the sandwich beam

IV.3.4. Step

within a model we define a sequence of one or more analysis steps, the step sequence provides a convenient way to capture changes in the loading and boundary conditions of the model, changes in the way part of the model interact with each other, and any other changes that may occur in the model during the course of the analysis, in addition, steps allow us to change the analysis procedure, the data output, and various controls, we can also use steps to define linear perturbation analyses.

IV.3.5.Load

this process allows as putting and controlling the type of charge (concentrated force, moment, pressure ...) and also put the convenient boundary condition on sandwich beam. We restrain one and of the sandwich beam and the other are free

IV.3.6. Boundary condition

[One restrained tip with tow face sheets has a regulare shape]

Table.IV.4. boundary condition

clamped (x=0)	Free (x=L)
$U_1 = U_2 = U_3 = 0$	$\frac{\partial^3 w}{\partial x^3} = 0 = Q$
$\theta_1 = \theta_2 = \theta_3 = 0$	$\frac{\partial^2 w}{\partial x^2} = 0 = M$

We get

Figure IV.5. Concentrated force in the sandwich beam

IV.3.7. mesh

a mesh is an arrangement of finite elements defined on an FEA model, in ABAQUS/CAE we can define a mesh on a part or on the assembly. Mesh is the activity of discretizing into a finite element representation**.**

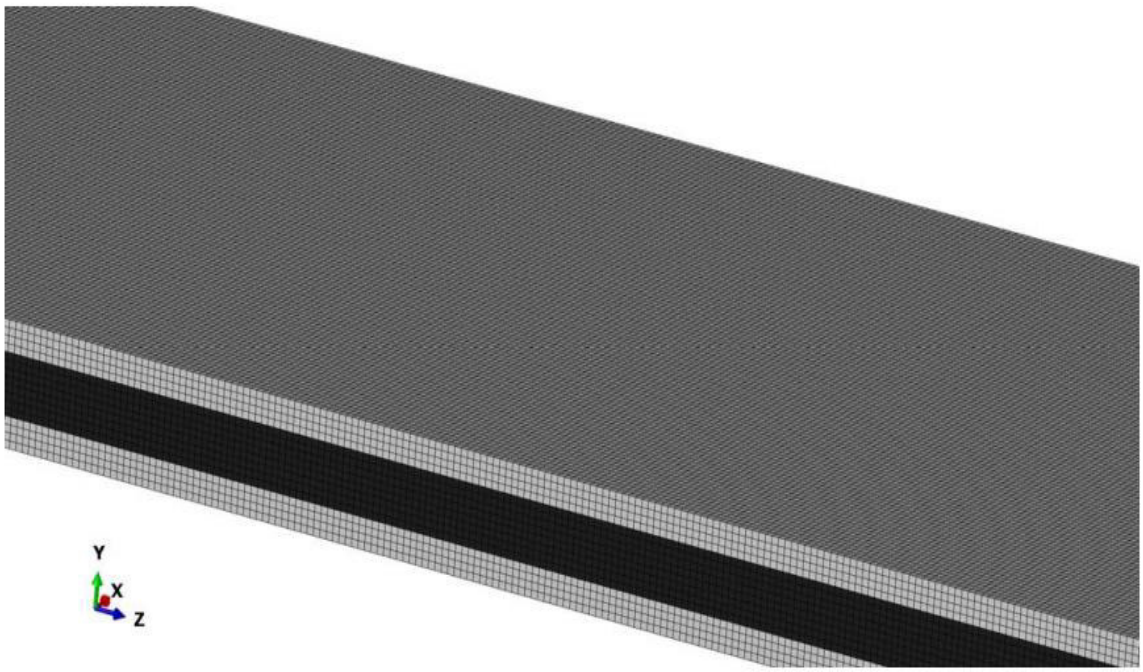

Figure IV.6. The sandwich beam is meshed

IV.3.8. problem size

Global seeds have been assigned.

576000 elements have been generated on instance: Part-1-1

576000 elements have been generated on instance: Part-2-1

1152000 elements have been generated on instance: Part-3-1

IV.3.9. Job

Thanks to this process we can easily start the submit that calculates the stress, strain, frequencies ....etc.

IV.3.10. Visualization

the visualization module provides graphical of finite element models and result, it obtains model and result information from the output database, major capabilities of the visualization

modul include in reformed and deformed shape plotting, results contour and symbol plotting X-Y plotting and reporting, field output reporting, plot customization and animation.

IV.4. Numerical results and discussion

in this three figures (8-10) we see that Abaqus result with finite element method show us that the high value of elongation is situated on the side of sandwich beam who we are applied forces, we shows this with red color, where it is fixed on the other hand of the sandwich beam.

Component U3 (0.1T)

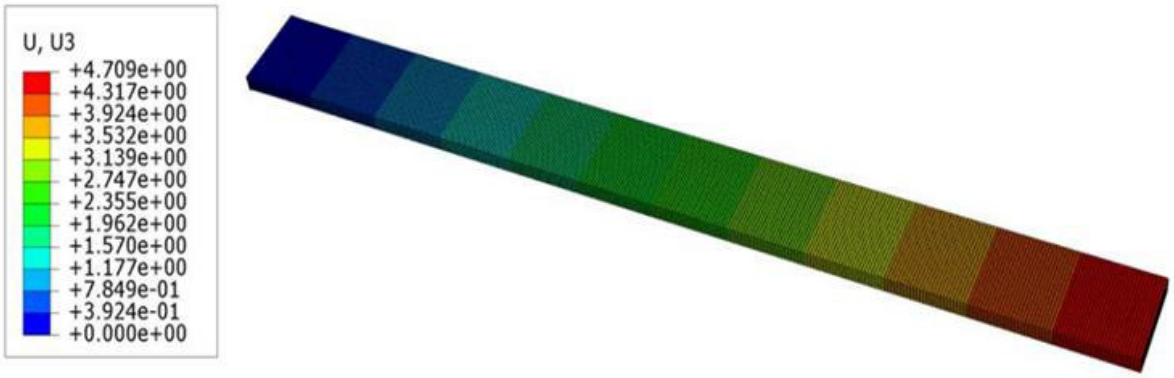

Figure IV.7. The elongation in the sandwich beam with deformation scale factor +6,371e^{+00}

Component U3 (0.5T)

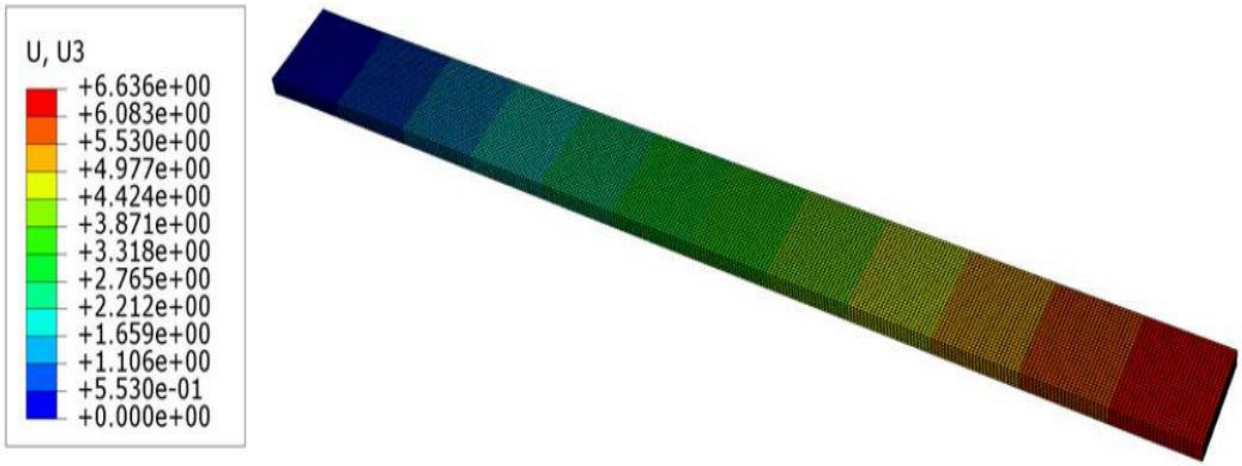

Figure IV.8. The elongation in the sandwich beam with deformation scale factor $+3{,}688e^{+00}$

Component U3 (0.3T)

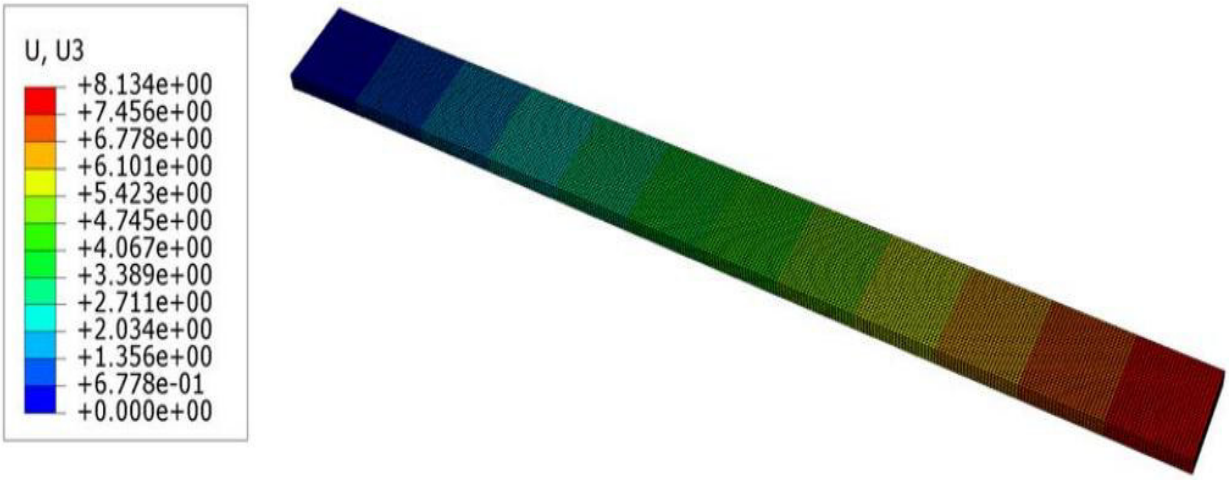

Figure IV.9. The Elongation in the sandwich beam with deformation scale factor $+4{,}521e^{+00}$

Table.IV.5. results of figure 8.9.10

component	U3-1	U3-2	U3-3
Max Elongation	$+4{,}709e^{+00}$	$+6{,}636e^{+00}$	$+8{,}134e^{+00}$
Min Elongation	0	0	0
deformation scale factor	$+6{,}371e^{+00}$	$+3{,}688e^{+00}$	$+4{,}521e^{+00}$

IV.4.1. Deduction

We observe that the major elongation occurs on the side even other side face at it is fixed (encastre) and (when there are reaction force), contrary the deformation occurs mainly in the viscoelastic core, and From these components we see that elongation is different within the sandwich beam.

IV.4.2. Ritz results

In this Figures 11.12.13 shows the variation of the elongation (mm) as a function of traction forces (N) of resonance of the beam under the influence of a magnetic field ranging from 0T to 0,5t.with method of Ritz

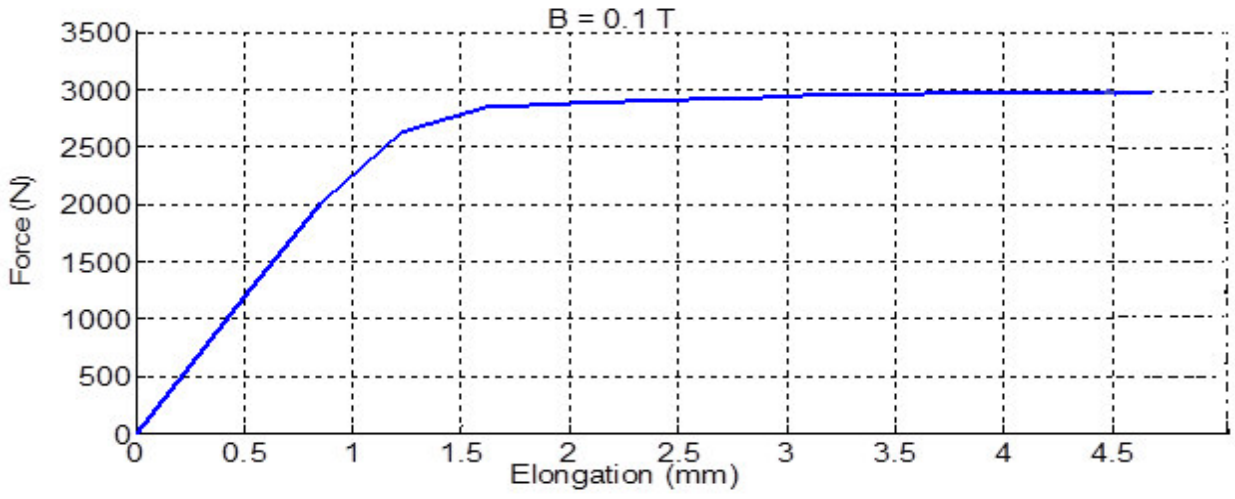

Figure.IV.10. variation of force as function of elongation with B=0,1T

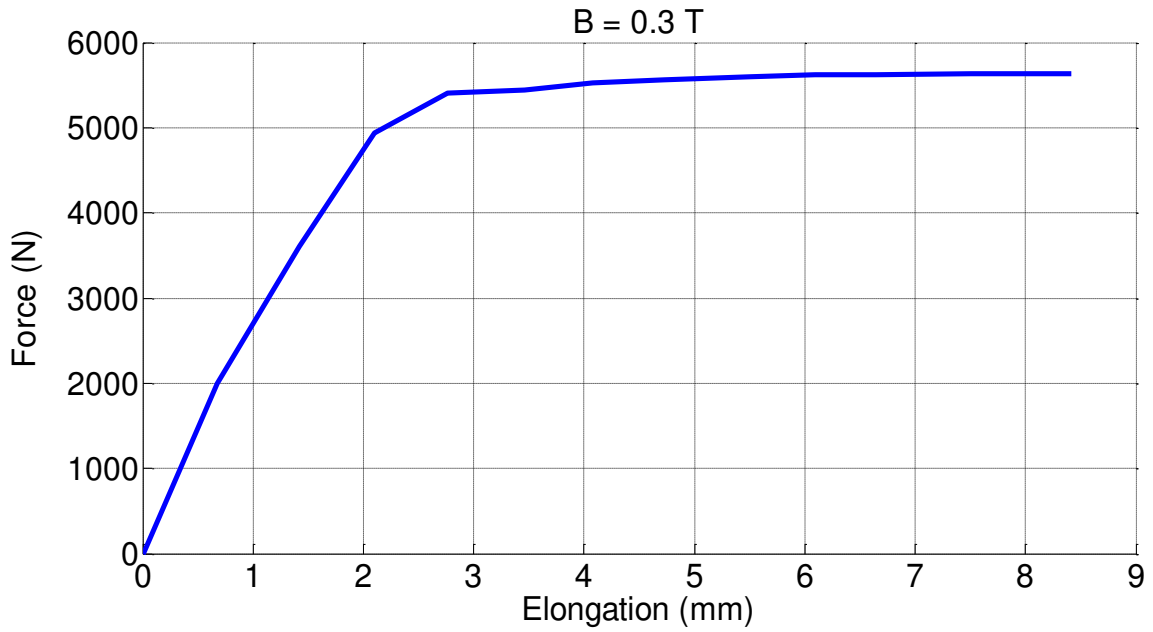

Figure.IV.11. variation of force as function of elongation with B=0,3T

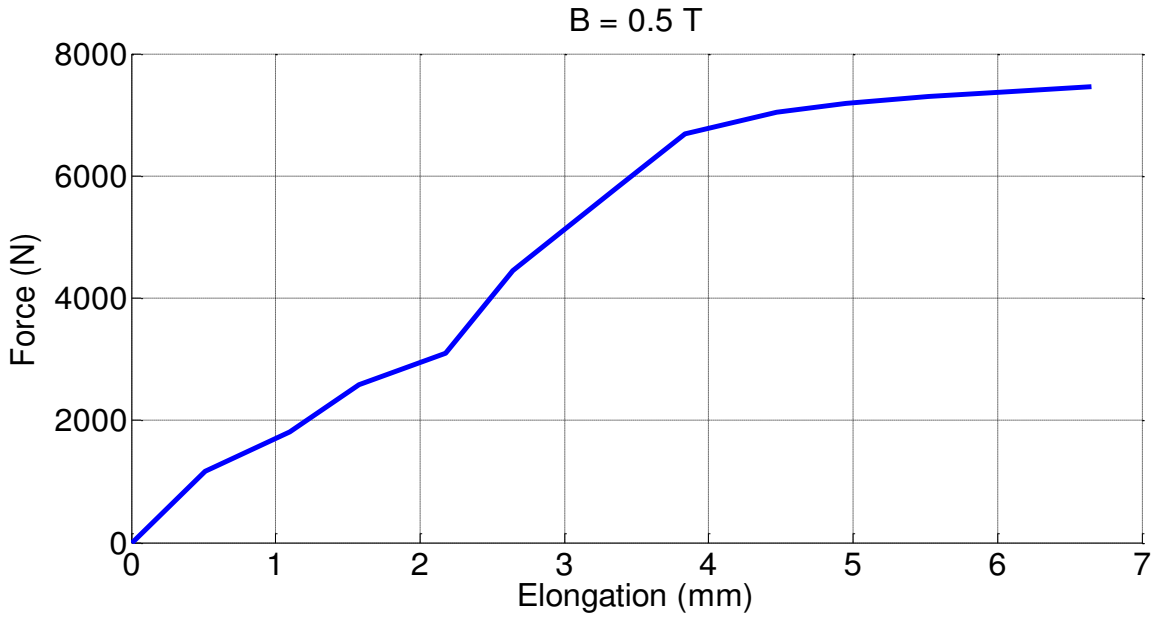

Figure.IV.12. variation of force as function of elongation with B=0,5T

Table.IV.6. results of Ritz method corves

MFI	Ultimate forces Point	Upper yield forces Point	Elongation in Upper yield forces Point
B=0,1T	3000 N	2700 N	1.2 (mm)
B=0,3T	5600 N	5000 N	2.1 (mm)
B=0,5T	7500 N	6900 N	3.8 (mm)

IV.4.2.1. Deduction

Table of results represent variation of forces-elongation versus under the excitation magnetic field intensity (B=0.1, B=0.3, B=0.5). We used the Ritz method and we see the elongation increase as the increasing of magnetic field intensity because, the increasing of magnetic field caused the increasing of the MRE stiffness,

IV.4.3. ABAQUS results

In this Figures 14.15.16 shows the variation of the elongation (mm) as a function of traction forces (N) of resonance of the beam under the influence of a magnetic field ranging from 0T to 0,5t, with method FEM (ABAQUS)

.

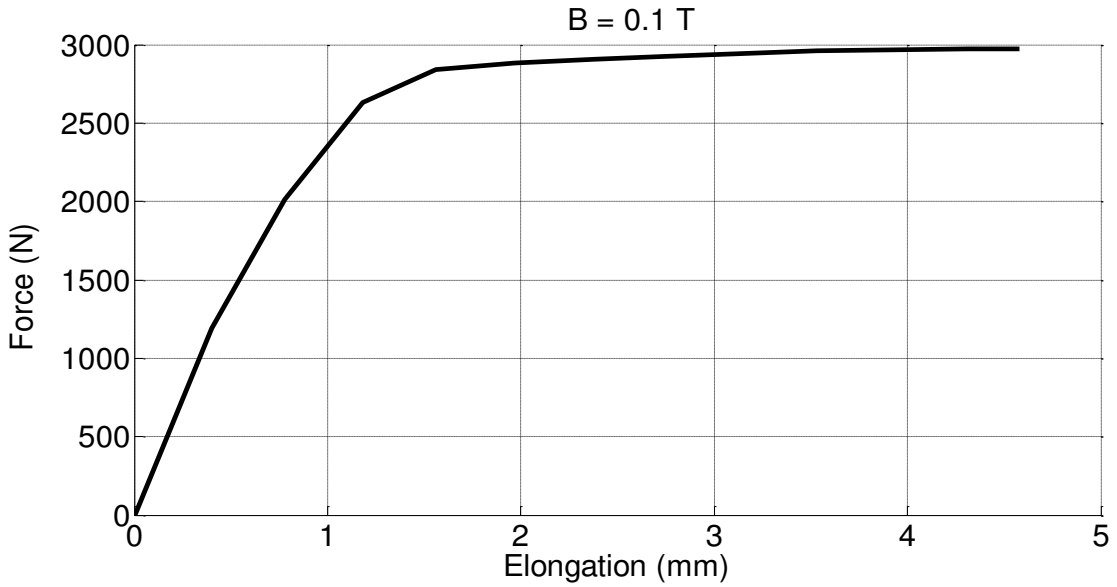

Figure.IV.13. variation of force as function of elongation with B=0,1T

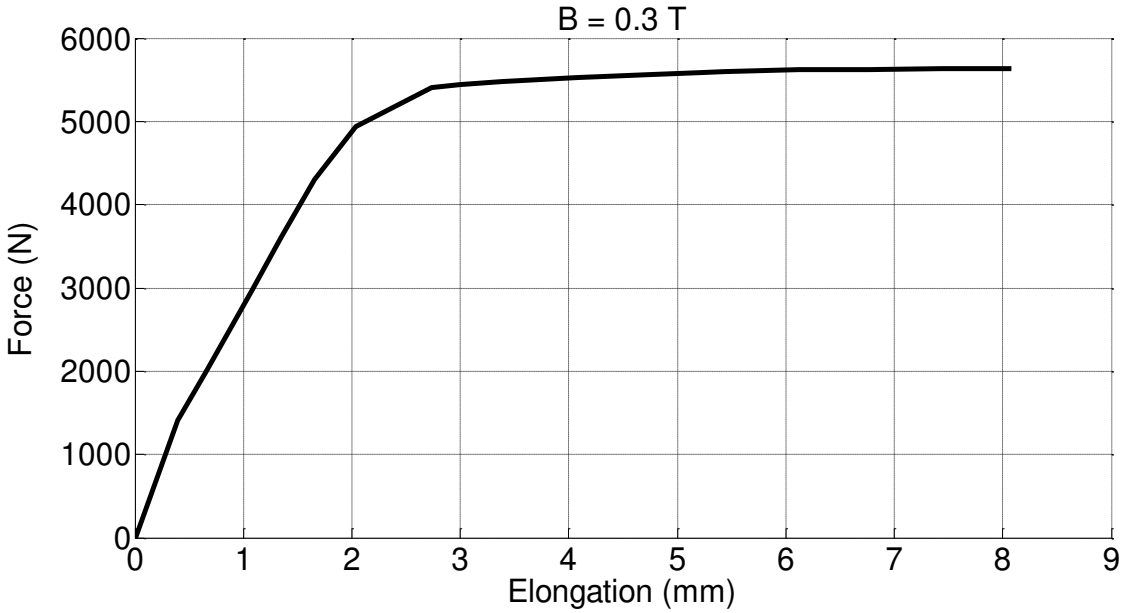

Figure.IV.14. variation of force as function of elongation with B=0,3T

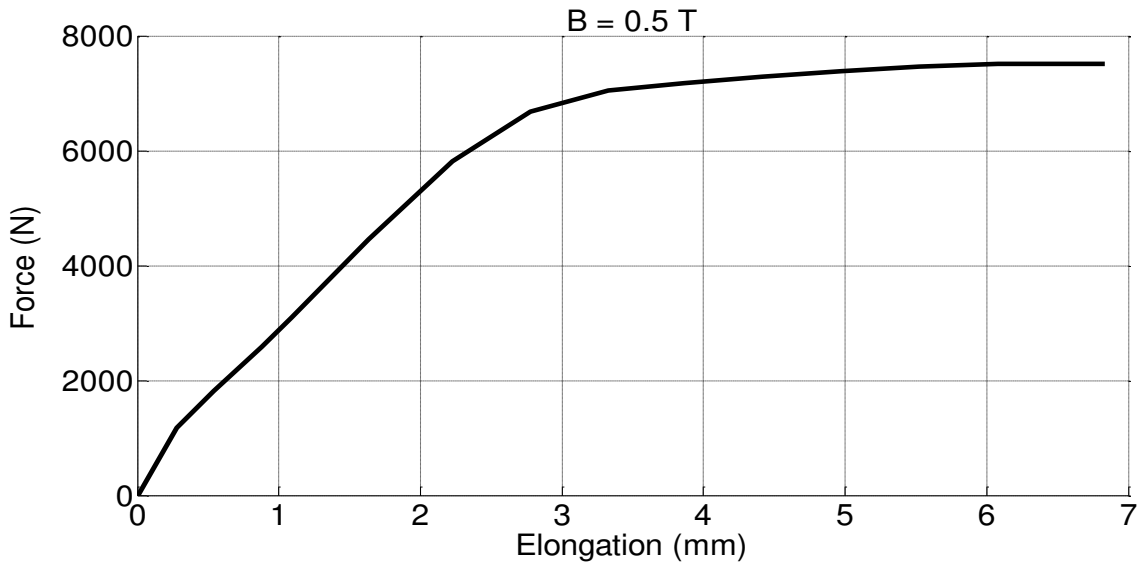

Figure.IV.15. variation of force as function of elongation with B=0,5T

Table.IV.7. results of Abaquz corves

MFI	Ultimate forces Point	Upper yield forces Point	Elongation in Upper yield forces Point
B=0,1T	3000 N	2700 N	1.2 (mm)
B=0,3T	5600 N	5000 N	2 (mm)
B=0,5T	7500 N	6900 N	2.9 (mm)

IV.4.3.1. Deduction

Abaquse results corves represents the variation of forces-elongation curves of the sandwich beam in deferent magnetic field intensity (B=0.1,B=0.3,B=0.5),we can observe the Ultimate forces and Upper yield forces varied proportionally with magnetic field intensity variation, the increasing of magnetic field intensity caused the increasing of the MRE stiffness,

IV.4.4. Comparison of ritz corves with abaqus corves

In figures 17, 18 and 19 We compare the results corves of forces-elongation of ritz method and ABAQUS by finite element method, the Black corves represent the abaqus results and the blue corves represent the ritz method results , under the excitation magnetic field intensity (B=0.1, B=0.3, B=0.5).

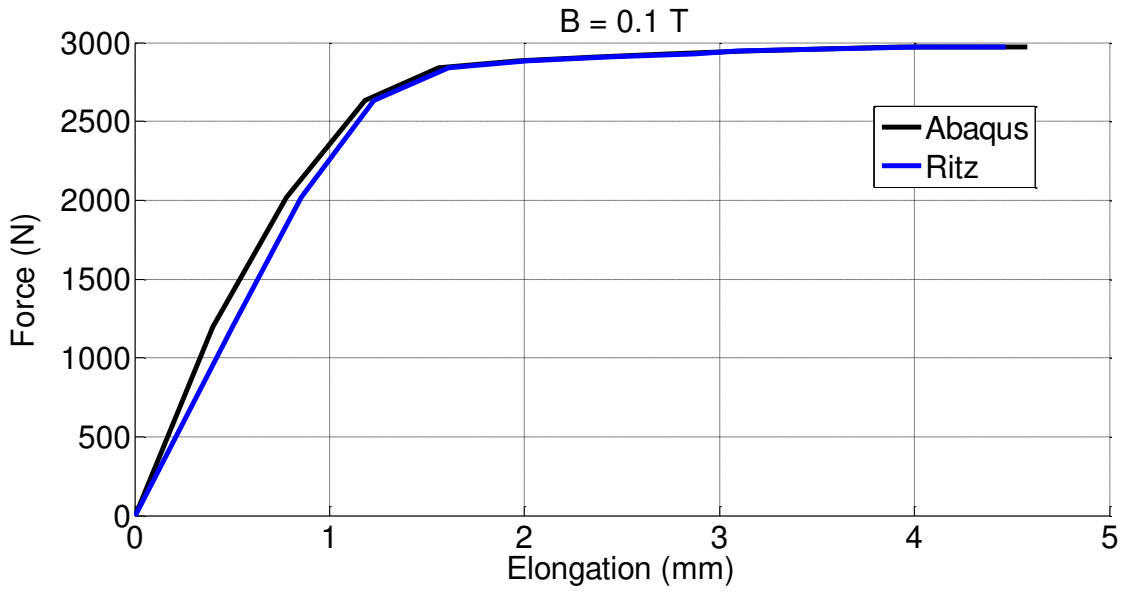

Figure.IV.16. Comparison of ritz corve with abaqus corve with B=0.1T

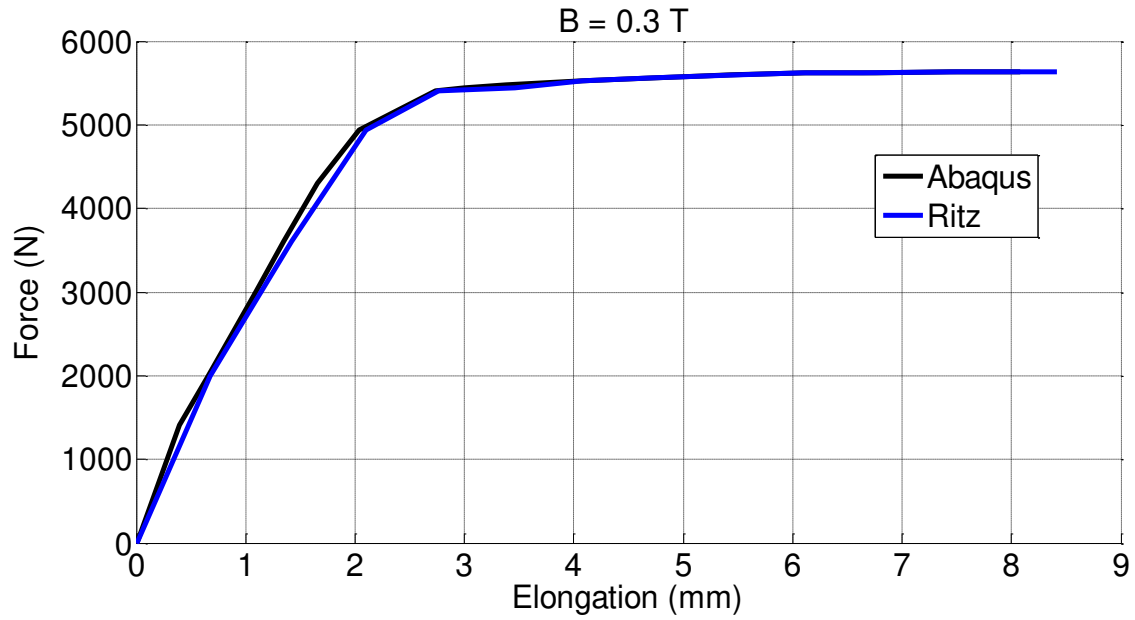

Figure.IV.17. Comparison of ritz corve with abaqus corve with B=0.3T

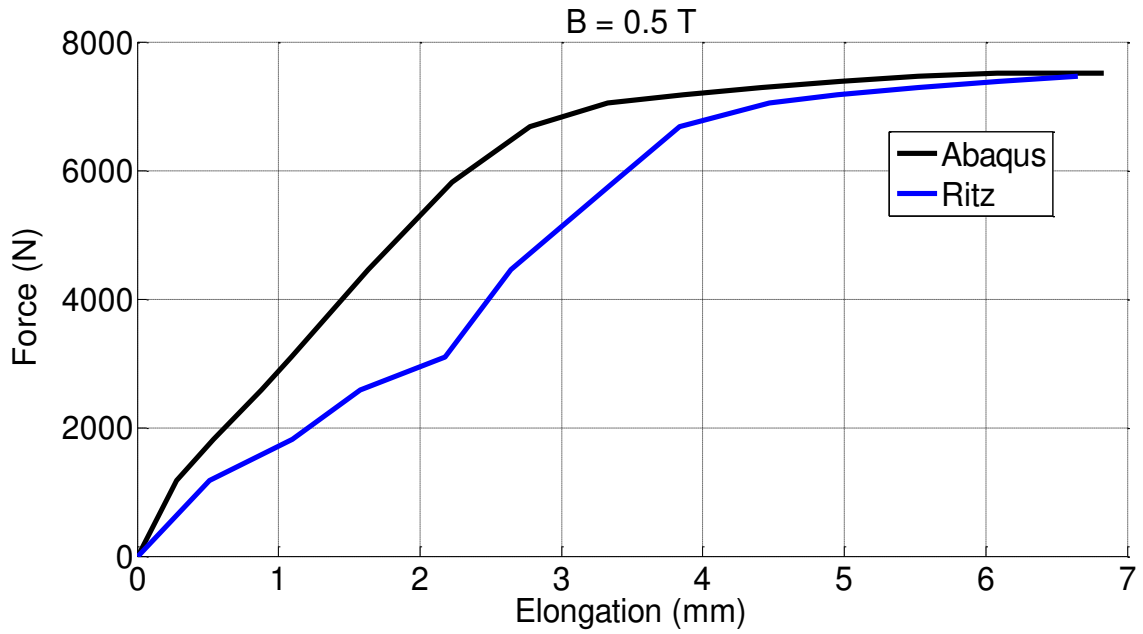

Figure.IV.18. Comparison of ritz corve with abaqus corve with B=0.5T

IV.4.4.2. Deduction

For magnetic field intensity of B=0.1T and B=0.3T the results between Ritz method and abaqus it is almost similar but for magnetic field intensity of B=0.5T we had different values ,where shows as the results in abaqus the MRE stiffness stronger than in Ritz method , where in really the comparison Must always to be similar.

IV.5. Conclusion

This article was devoted to the experimental and numerical analysis of elongation response of a magneto-rheological elastomer sandwich beam without and under the influence of deferent values of the force, subjected to harmonic excitation by a magnetic field, the numerical and experimental tests were conducted on a sandwich beam with a charge rate 40% of the elastomer by the micro particles of iron to a highlighted an intelligent control for traction forces, the forces dependence and magnetic field of the viscoelastic behavior of magneto rheological elastomer introduces complexity in direct and accurate determination of the stiffness proportie and prediction of elongation response of the beam.

Experimental and numerical results allowed drawing the following conclusion:

- In the presence of elongation, the beam characteristic not stabilized under the influence of the magnetic field, even at variable forces.
- For the incorporation of a layer of elastomer charged by the iron particles in a magnetic field, increases the rigidity without losing the characteristics due to the viscous damping properties of the elastomer.
- The influence of iron charges increases the mechanical characteristics of the elastomer particularly the stiffness by creating attractive forces between the iron particles.
- The stiffness and the loss factor can be adjusted in an intelligent manner based on any probable solicitation.

Finally, these new structures magneto-rheological (beams or plates), with many potential applications in all industries, especially the building, to develop a functional composite material with good elongation and damping properties, it is important to monitor rheological properties and the magneto-rheological effect. Rheological properties depend on the amount of ferromagnetic particles and their arrangement.

CHAPTER IV

Numerical simulation and comparison results

General conclusion

The purpose of this research work is devoted to make a contribution on the determination of the dynamic response of beams sandwiches with a heart in Mgnetorheogical elastomers.

in this research work the objectives focused on the solution of traction problem in sandwich beam with MRE core and two isotropic face sheets and provide a basic know ledge of constrained layer viscoelastic damping material to apply in aerospace application while considering customer requirement such as cost, weight, environmental facture, and dumping effectiveness, first we investigate about viscoelastic and MRE materials and its different properties then we represent some useful classical and modern damping models, in this study elongation treatment has been applied to asymmetric sandwich beam, this work has also been extended to finite element analysis of traction structure to show the elongation response or harmonic response.

We have seen that the introduction of a viscoelastic layer dumping between two faces sheets can produce a structure with high damping and this sandwich structure have the additional advantage that their strength to weight ratio also the core increase the thickness of the structure, which lead to an increase in stiffness of the sandwich structure. We have used a finite element method (FEM) to determine the statec and dynamic response of the sandwich beam, we used rayliegh-ritz method, method was developed for the sandwich beam analyses, in this research, the static strain-stress relationship was studied, static and Dynamic properties of thin sandwich structure with viscoelastic core were discussed in this dissertation, for the sandwich beam the necessary static and dynamic parameters can be now estimated. The expression of the elongation number and speed of traction elongation in sandwich beam were obtained, bases on both static and dynamic studies, the elongation dependence of traction was analyzed for a viscoelastic MRE sandwich beams, in which the face sheets are much thinner than the core, or the structural parameter is large, it was found that if the magnetic field intensity increase in MRE the stiffness increase and transverse displacement decrease in static force, the non-linear change of the rheological properties in MRE was found, we studied analysis of vibration response of a MRE sandwich beam under excitation of magnetic field and influence of different values of the forces , found that the MRE rapidly stabilized under the influence of the magnetic field.

The experimental results of the dynamic and static tests of the MRE samples cured without and under magnetic field were presented and compared in the paper. The influence of the MRE internal structure and external magnetic field on the researched strength parameters was strictly proofed.

[1] W. Flugge, "viscoelasticity", 2nd ed, springer, berlin, 1975.

[2] Yzhou and Y L zhang, optimal design of a shear magnetorheological damper for turning vibration suppression, smart mater. Struct. 22(2013) 0964-1726

[3] Z. G. Ying, Y.Q. Ni, S. Q. Ye, stochastic micro-vibration suppression of a sanswich plate using a magnetorheological viscoelastomer core, journal of smart materials and structures. 23(2014)025019 (11pp)

[4] S. K. Dwivedy, N, mahendra, K.C. Sahu, parametric instability regions of a soft and magnetorheological elastomer cored sandwich beam, journal of sound and vibration 325 (2009) 686-704.

[5] Marie E. Rognes "mixed finite element method with application to viscoelasticty and gels" (2009)

[6] Culshaw, B., smart structures and material, artech house Inc, 1996 and bank, H. T., smith, RC. And wang, Y., smart material structures, modeling, estimating and control, john wiley and sons, 1996

[7] Dufault, F. And akhras, G., applications of smart material and structures in bridge construction, proceedings, 3rd cansmart workshop on smart materials and structures, sep.2000,pp. 149-159.

[8] Y. Wang, D. J. Inman, Finite element analysis and experimental study on dynamic properties of a composite beam with viscoelastic damping, Journal of Sound and Vibration. 332(2013) 6177-6191.

[9] Ya Wang, Daniel J. Inman, Finite element analysis and experimental study on dynamic properties of a composite beam with viscoelastic damping, Journal of Sound and Vibration, 332(2013) 6177-6191.

[10] S.K. Dwivedy, N. Mahendra, K.C. Sahu, Parametric instability regions of a soft and magnetorheological elastomer cored sandwich beam, Journal of Sound and Vibration 325(2009) 686-704

[11] Lu Ean Ooi, Zaidi Mohd Ripin, Dynamic stiffness and loss factor measurement of engine rubber mount by impact test, Materials and Design 32(2011)1880-1887.

[12] L yancheng, L jianchun, T tian and L weihua, A highly adjustable magnetorheological elastomer base isolator for application of real-time adaptive control, smart mater. Struct. 22(2013)0964-1726.

[13] SULLIVAN J., DEMERY V., "The nonlinear viscoelastic behaviour of a carbon-blackfilled elastomer", Journal of Polymer Science: Polymer Physics Edition, 20 (1982) 2083-2101

[14] LIANG J., LI R., TJONG S., "Effect of glass bead content and surface treatment on viscoelasticity of filled polypropylene/elastomer hybrid composites", Polymer International, 48 (1999) 1068-1072

[15] DEMCHUK S., KUZ'MIN V., "Viscoelastic properties of magnetorheological elastomers in the regime of dynamic deformations", Journal of Engineering Physics and Thermophysics, 75, **2** (2002) 396-400

[16] ZHOU G., "Shear properties of a magnetorheological elastomer", Smart Materials and Structures, 12 (2003) 139-146

[17] ZHOU G., LI J., "Dynamic behaviour of a megnetorheological elastomer under uniaxial deformation: I. Experiment", Smart Materials and Structures, 12 (2003) 859-872

[18] Carlson J.D., Jolly M.R., MR fluid, foam and elastomer devices, Mechatronics, 10:555-569, 2000.

[19] Farshad M., Benine A., Magnetoactive elastomer composites, Polymer Testing 23: 347-353, 2004.

[20] Zhou G.Y., Shear properties of magnetorheological elastomer, Smart Materials and Structures 12:139-146, 2003.

[21] Tumanski S., Handbook of Magnetic Measurements, CRC Press Taylor & Francis Group, 2006.

[22] Fiorillo F., Measurement and characterization of magnetic materials, Elsevier Academic Press, 2004.

[23] Valery P. Mikhailov, Alexey M. Bazinenkov, Active vibration isolation platform on base of magnetorheological elastomers**,** Journal of Magnetism and Magnetic Materials, Volume 431, 1 June 2017, Pages 266-268

[24] Mirosław Bocian, Jerzy Kaleta, Daniel Lewandowski, Michał Przybylski, Tunable Absorption System based on magnetorheological elastomers and Halbach array: design and testing**,** Journal of Magnetism and Magnetic Materials, Volume 435, 1 August 2017, Pages 46-57

[25] Mateusz Kukla, Jan Górecki, Ireneusz Malujda, Krzysztof Talaśka, Paweł, Tarkowski, The Determination of Mechanical Properties of Magnetorheological Elastomers (MREs)**,** Procedia Engineering, Volume 177, 2017, Pages 324-330

[26] Guojiang Liao, Yangguang Xu, Fengjun Wang, Fayuan Wei, Qiang Wan, Influence of γ radiation on the shear modulus of magnetorheological elastomer **,**Materials Letters, Volume 174, 1 July 2016, Pages 79-81